2019-12-13

A Role for the Hypoxia-Inducible Factor 1 Alpha in Murine Gammaherpesvirus 68 (MHV68) Lytic Replication and Reactivation from Latency

Darlah Michelle López-Rodríguez
University of Miami, dlopezrodriguez@med.miami.edu

UNIVERSITY OF MIAMI

A ROLE FOR THE HYPOXIA-INDUCIBLE FACTOR 1 ALPHA IN MURINE GAMMAHERPESVIRUS 68 (MHV68) LYTIC REPLICATION AND REACTIVATION FROM LATENCY

By

Darlah Michelle López-Rodríguez

A DISSERTATION

Submitted to the Faculty
of the University of Miami
in partial fulfillment of the requirements for
the degree of Doctor of Philosophy

Coral Gables, Florida
December 2019

UNIVERSITY OF MIAMI

A dissertation submitted in partial fulfillment of
the requirements for the degree of
Doctor of Philosophy

A ROLE FOR THE HYPOXIA-INDUCIBLE FACTOR 1 ALPHA IN MURINE GAMMAHERPESVIRUS 68 (MHV68) LYTIC REPLICATION AND REACTIVATION FROM LATENCY

Darlah Michelle López-Rodríguez

Approved:

_____ Samita Andreanksy, Ph.D. Research Assistant Professor of Pediatrics	_____ Enrique Mesri, Ph.D. Professor of Microbiology and Immunology
_____ Wasif N. Khan, Ph.D. Professor of Microbiology and Immunology	_____ Ralf Landgraf, Ph.D. Associate Professor of Biochemistry and Molecular Biology
_____ Scott Tibbetts, Ph.D. Associate Professor of Molecular Genetics and Microbiology	_____ Guillermo Prado, Ph.D. Dean of the Graduate School

LÓPEZ-RODRÍGUEZ, DARLAH MICHELLE (Ph.D., Microbiology and Immunology)

A Role for the Hypoxia-Inducible Factor 1 alpha in Murine Gammaherpesvirus 68 (MHV68) Lytic Replication and Reactivation from Latency.

(December 2019)

Abstract of a dissertation at the University of Miami.

Dissertation supervised by Assistant Professor Samita Andreansky and Professor Enrique A. Mesri
No. of pages in text (99)

The hypoxia inducible factor 1 alpha (HIF1α) protein and the hypoxic microenvironment are critical for infection and pathogenesis by the oncogenic gammaherpesviruses (γHV) such as Kaposi' Sarcoma-associated Herpes Virus (KSHV) and Epstein-Barr virus (EBV). However, understanding the role of HIF1α during the virus life cycle and its biological relevance in the context of host pathogenesis has been challenging due to the lack of animal models for human γHV. To study the role of HIF1α we employed the murine gammaherpesvirus 68 (MHV68), a rodent pathogen that readily infects laboratory mice. We show that MHV68 infection induces HIF1α protein and HIF1α-responsive gene expression in permissive cells. Deletion of HIF1α reduces virus production due to a global downregulation of viral gene expression. Most notable was the marked decrease in many viral genes bearing hypoxia regulatory element (HRE)

such as viral G-Protein Coupled Receptor (vGPCR), which is known to activate HIF1α transcriptional activity during KSHV infection. Intranasal infection of HIF1α$^{LoxP/LoxP}$ mice with MHV68 expressing Cre-recombinase impaired virus expansion during early acute infection and affected lytic reactivation in the splenocytes explanted from mice. Moreover, low oxygen conditions accelerated lytic reactivation and enhanced virus production in MHV68 infected splenocytes. Thus, we conclude that HIF1α plays a critical role to promote virus replication. Our results highlight the importance of the mutual interactions of the oxygen-sensing machinery and gammaherpesviruses in viral replication and pathogenesis.

"This book,

more than a book, is a longing;

more than a longing,

an intention;

more than an intention,

it is thirst.

Thirst for justice and truth;

Intention to prove that there is further bliss than what men pursue:

Desire that the example bears fruit."

-Eugenio María De Hostos

"La peregrinación de Bayoán"

This doctoral dissertation to the field of Microbiology and Immunology is dedicated to the beautiful island of Puerto Rico and the victims of Hurricane María in 2017.

ACKNOWLEDGMENTS

I would like to thank my mentors, Dr. Samita Andreanksy and Dr. Enrique Mesri. I am grateful for your patience and understanding. I feel privileged to have worked under your tutelage in a fascinating subject which combined both your expertise. I would like to thank my advisor, Dr. Samita Andreanksy. I am so grateful from the day you took me under your wing and taught me to love viruses, manage a wet-laboratory and insisted I seek graduate studies. Thank you, Samita, for trusting me to be part of your lab from the beginning. Thank you for guidance and your patience. Next, I would like to thank my second advisor, Dr. Enrique Mesri for whom I have tremendous respect as a scientist. Thank you for allowing me the opportunity to carry on a fascinating research project in your laboratory and forgiving my mistakes. I am grateful to you for being patient, compassionate and kind.

To past lab members Annalise Smith, Sarah Rodríguez, Andrea Correa, Zhanna Kozhekbaeva, Brittany Ashlock, Howard Leung, and Lucas Cavallin. To present lab members, Julian Naipauer, Mariana Schlesinger, Carolina Alvarez and Mourad Bendjennat. Thank you for your kind disposition and helping with every aspect of laboratory life and everything KSHV. I feel so lucky and grateful to have worked with such amazing people. You made my days brighter.

To my beautiful and wonderful friends, Santas Rosario, Steven Grieco, Kinsley Belle and Omayra Méndez Solis. It is difficult to articulate how important you were throughout this journey. Thank you for your emotional support and believing in me.

To my boyfriend Giovanni Mastrogiovanni and the love of my life, my dog, Noodles. Thank you for bringing so much joy into my life in the best and difficult moments.

To my mother, my father, my brother, Gaby and my sister, Alexandra, its wasn't easy but we made the best of it. I love you.

Finally, to my great-aunt Carmen D. Rodríguez Marrero. Thank you for always encouraging me to pursue my goals since I was a child. I am forever grateful to you and all you taught me. Thank you for teaching to be loud and proud of being Puerto Rican.

TABLE OF CONTENT

LIST OF FIGURES

PUBLICATION NOTE

Chapters 1-5:

Versions of some material within these chapters are published in:

López-Rodríguez DM, Kirillov V, Krug LT, Mesri EA, Andreansky S (2019) A role of hypoxia-inducible factor 1 alpha in Mouse Gammaherpesvirus 68 (MHV68) lytic replication and reactivation from latency. PLoS Pathog 15(12): e1008192. https://doi.org/10.1371/journal.ppat.1008192

CHAPTER 1

INTRODUCTION

1.1. An Overview of the Herpesvirus family

Herpesviruses have been around for a very long time. The typical herpes virion morphology and DNA replicative system of those found in the present-day can be trace 400 million years ago infecting birds and reptiles (McGeoch et al. 1995). A typical herpesvirus particle consists of a linearized double-stranded DNA molecule of 100 to 200,000 base pairs long contained in an icosahedral capsid of approximately 120 to 125 nm in diameter. Viral proteins associated with the tegument layer between the capsid and the viral envelope carry out immediate functions when deposited upon infection of the cell. Finally, the lipid envelope is composed of virally encoded glycoproteins that grant cell entry. Once inside the cell, herpesviruses infer their biological fate on the state of infection and how well it subdues immune detection.

The family of large dsDNA viruses shares a persistent lifestyle, also known as a latent phase or latency program, which grants the benefit of surviving inside the cell without genomic integration but as a viral episome tethered to the host chromosome. Latency is also characterized by the

transmission of the viral genome to inconspicuous daughter cells without producing any infectious particles. Only a handful of viral proteins are present which inhibit apoptosis while enhancing cell survival and proliferation. The switch to lytic infection, also known as herpesvirus reactivation, leads to virus replication, but the genome is packaged and disseminate as viral particles go and infect other cells or another host. Lytic replication occurs in a self-regulated cascade of gene expression, beginning with an accumulation of immediate-early mRNA (α-genes), which occurs independently of de novo protein synthesis. Their products manage many cellular functions, including cell cycle, apoptosis, metabolism, and immune response (Fields and Knipe 2013). Also, they initiate the expression of the next batch of early genes or β-genes. These genes begin viral genome replication. Multiple copies of the genome are synthesized continually in rolling-circle replication in the nucleus. Lastly, γ-genes or late genes involved encode structural and virion-associated proteins for viral particle assembly in the cytoplasm. The initiation of this cascade does not always result in the replication, also referred to as abortive infection (**Figure 1.1.1**).

Fig. 1.1.1. Herpesvirus lifecycle. Once the infection is initiated, it can either proceed to lytic or latent replication. On the other hand, lytic replication results in the production of virions and cell lysis.

However, not all infection reads to genome replication. In an abortive infection, several of the immediate-early gene arrays are expressed. Lytic genes will be repressed, depending on the state of infection and advancement in antiviral responses, and establishing latency. The viral products associated with this lifecycle regulate cell survival and apoptosis. The herpesvirus genome persists in the host by duplicating along with cell mitosis.

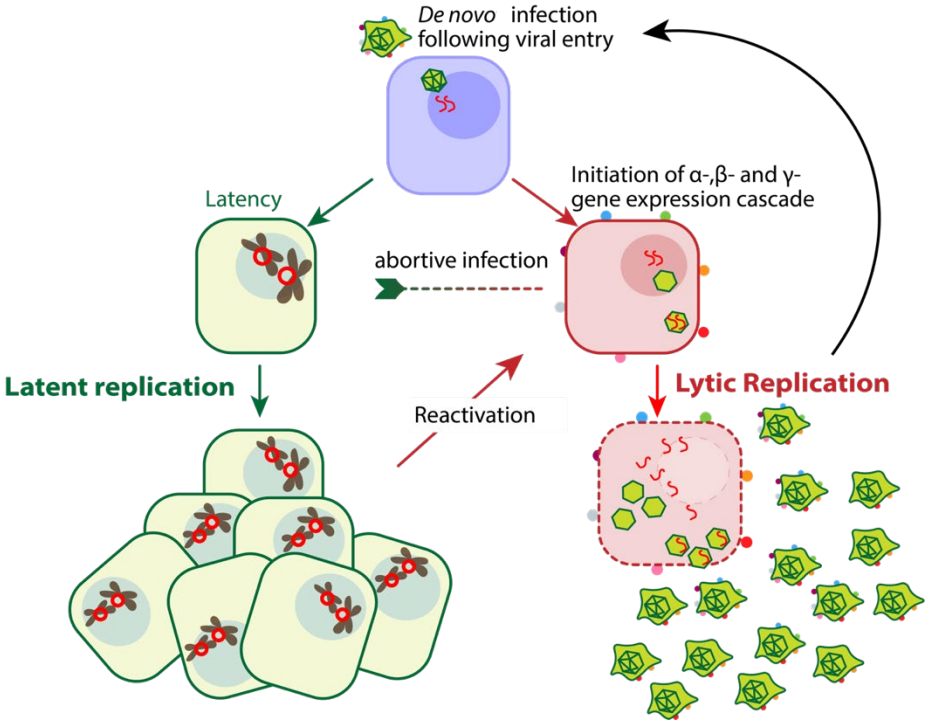

Herpesviruses divide into three subfamilies, alpha-, beta- and gammaherpesviruses. Alphaherpesviruses infect a wide range of host species, from reptiles, birds, even mollusks, and have been around the longest. The most common alpha-herpesvirus infecting mammals is Herpes Simplex-1, manifesting as cold-sores and Varicella Zoster, also known as chickenpox or shingles. Both establish latency in neuronal cells. Members of the betaherpesviruses have a restricted species range, infecting elephants, non-human primates, and humans. However, they have broader cell tropism, for example,

human cytomegaloviruses can infect hematopoietic and epithelial cell types. Finally, the subfamily of gammaherpesviruses (γHVs) are lymphotropic, highly host-restricted, and mammals are the only natural host. Its emergence took place in the last 80 million years, probably with a significant component of cospeciation with primate lineages (McGeoch et al. 1995).

1.1.1. Introduction to the Gammaherpesvirus subfamily

The Epstein-Barr Herpesvirus (EBV) and the Kaposi' sarcoma-associated Herpesvirus (KSHV) are γHVs for which humans (homo sapiens) serve as hosts. They sustain clinical relevance due to their capacity to promote the cellular transformation of infected cells leading to tumorigenesis in setting where the host is immunocompromised. EBV classifies under the lymphocryptovirus genus, or gamma-1 herpesvirus, diverging from KSHV under the rhadinovirus genus, also known as gamma-2 herpesvirus (**Figure 1.1.2**). While they share the capacity for long-term latency establishment in the B-cell compartment, EBV infects many epithelial cell types and is associated with B-cell, and epithelial tumors with complex roles in NK- and T-cell lymphomas. On the other hand, KSHV is known to cause tumors of endothelial as well as B-cell origin. Both access B-lymphocytes by infection of naïve B-cells which

then triggers germinal center B-cells expansion. Once they reach mature B cells, the virus induces differentiation to a memory profile and plasmablasts B cells and ensures latency in a long-lived cell. One striking difference between these gamma-1 and gamma-2 herpesvirus is their mechanism of tumorigenesis. Sole expression of viral genes associated with the latency program of the lymphocryptovirus genus can cause cell transformation of B-cells. On the other hand, genetic polymorphisms, secondary infections, and environmental factors contribute to cellular transformation in the rhadinovirus genus, and both lytic and latency-associated genes are necessary (E. Mesri, Cesarman, and Boshoff 2010).

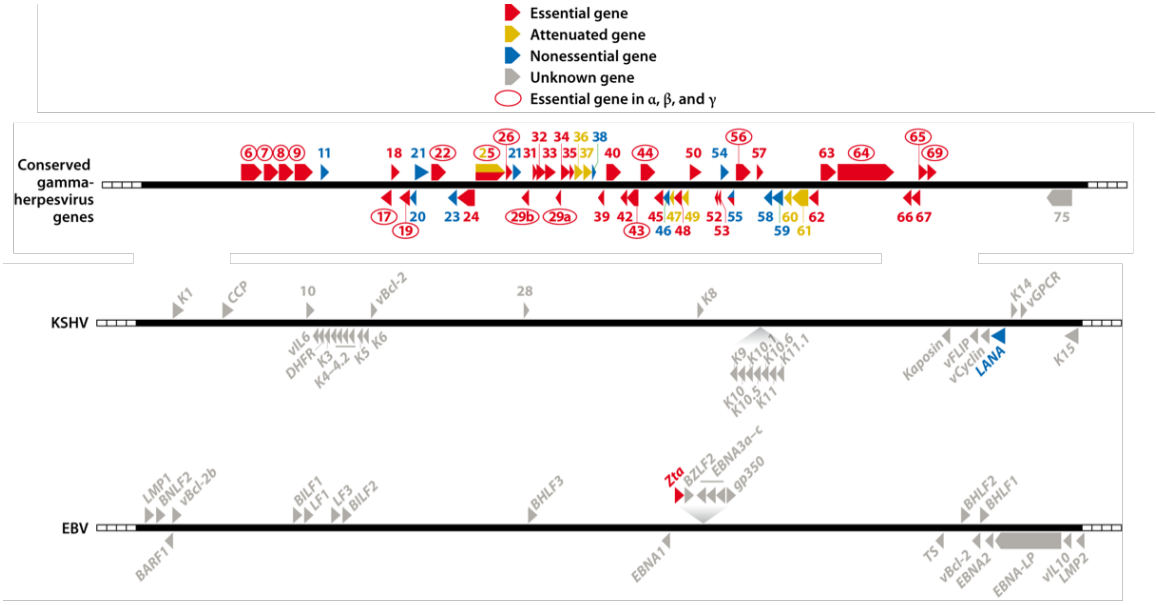

Fig. 1.1.2. Comparison of human gammaherpesviruses. Large blocks of the genome in the human gammaherpesviruses discussed in this chapter have conserved sequences and functions. They also contain unique genes (gray) specific for each virus.

EBV infection is quite common around the world and highly transmissible by saliva. More than 90% of the world's population is infected by adulthood, without signs or symptoms. A manifestation of an acute infection in western countries is the infectious mononucleosis (IM) syndrome. While highly ubiquitous, some associated cancers affect specific demographics suggesting a role for the prevalence of strain genetic variation. Nasopharyngeal carcinoma (NPC) commonly arises in infected individuals of Southern China, and the Sub-Saharan African region has a high incidence of Burkitt's lymphoma (BL). In contrast, KSHV infection is endemic within populations from the Mediterranean basin and Sub-Saharan Africa and quite rare in the rest of the planet until the beginning of the HIV epidemic. These moments in US history revealed that KSHV was found in skin tumor lesions of HIV-infected individuals but described almost two centuries before as Kaposi’ Sarcoma common in elderly Jewish men on the other side of the world.

1.1.2. Genetic organization and replication

The genetic organization of γHVs is highly conserved; however, there is no apparent homology in the DNA sequence. Nonetheless, they share the same function (viral orthologs),

inhibit apoptosis while promoting cell survival and proliferation. In KSHV, the primary latency transcripts consist of several proteins originating from the same genomic region under the latency-associated nuclear antigen (LANA) constitutive promoter, ORF73, ORF72, ORF71, Kaposin, and K12. LANA (ORF73) is essential, which the primary function is anchorage to the host chromosome during latency. Its tethering counterpart in EBV is the EBV-associated nuclear antigen-1 (EBNA-1), in addition to the latency-associated membrane proteins predominate during latency establishment but exert constitutive proliferative signaling. Chromatinization of the viral genome represses and regulates transcription of master lytic activator proteins. Treatment of lymphoma-derived cells with histones deacetylase inhibitors can induce the switch to lytic replication. The replication and transcription activator gene, RTA (ORF50) drives DNA replication and reactivation in KSHV, in addition to other regulatory functions in the host. In EBV, reactivation is led by expression of the two immediate-early genes, Zta (BZLF1) and Rta (BRLF1).

1.2. Gammaherpesvirus-associated malignancies

Most animals do not manifest illness due to a gammaherpesvirus infection, and being a carrier can favor

immunity in a host against specific bacterial pathogens (E. S. Barton et al. 2007). The faculty for remaining asymptomatic was acquired through millions and millions of years facing immune pressures by the host they inhabit. In distinction, DNA sequences of γHVs genome encode host homologs proteins that exert cellular functions that thwart detection at various levels of immunity. An imbalance that compromises host immunity, specifically immunosuppression, increases the risk of associated-malignancies. T-cell responses, specifically cytotoxic CD8+ and Natural Killer cells, control lytic replication, and reactivation from latency. This pressure selects for cells with a profile expression of latency-associated transcripts, which decreases immunogenicity by infection (**Figure 1.2.1**).

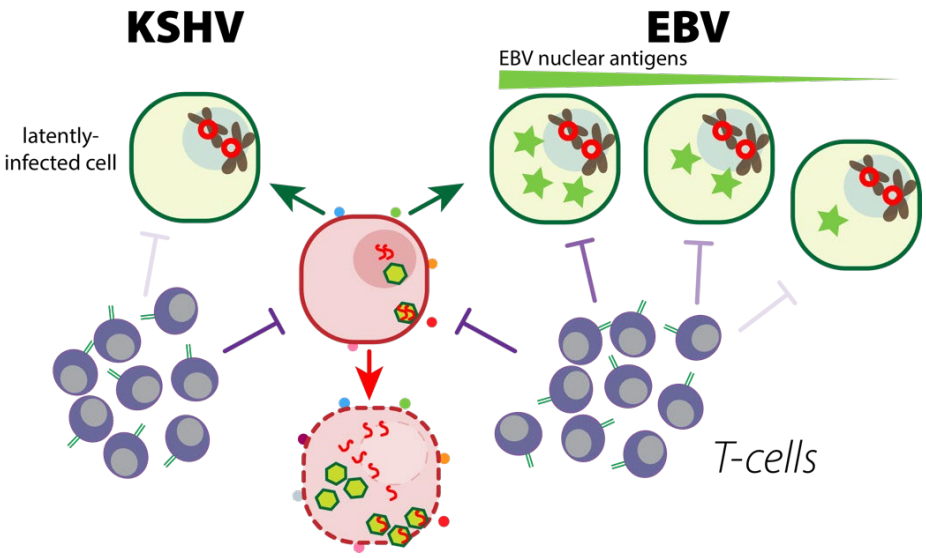

Fig. 1.2.1. Immunity by the host suppresses lytic infection and selects for latently infected cells. Cytotoxic CD8 T cells dampens lytic infection and immunogenic latently infected cells in healthy, immunocompetent individual.

1.2.1. Lymphomagenesis by gammaherpesvirus infection

Host immunosurveillance is crucial for controlling lytic replication and expression viral oncogenes, therefore clinically induced-immunosuppressive regimens following organ transplant increase the risk of post-transplant lymphoproliferative diseases (PTLD). A recent study spanning twenty years at the Mayo Clinic in Minneapolis revealed more than 60% of patients undergoing solid organ transplant and developed PTLD were positive for EBV infection when detected by in situ hybridization(Habermann et al. 2018). However, the incidence is higher in patients who are EBV negative at the time of transplantation and lack immunity against the virus (Cesarman 2013). These tumors are of B-cell origin, initially presenting enlarge and abnormal cytoplasm, or plasmacytic hyperplasia, a high infiltration of T-cells, also characteristic of infectious mononucleosis. Diffuse large B cell lymphoma (DLBCL), Hodgkin Lymphoma (HL), and Burkitt's Lymphoma (BL) in AIDS patients and HIV-infected individuals tend to manifest more aggressive phenotypes, but not exclusively (Figure 1.2.2.). The cellular modulatory activity of the different expression patterns of the EBV latency

programs are primers of oncogenesis. Moreover, several lytic genes possess oncogenic potential (E. A. Mesri, Feitelson, and Munger 2014). One study found the transcription of viral lytic reactivation correlated with cellular pathways involved tumorigenesis of EBV-immortalized LCLs (Arvey et al. 2012).

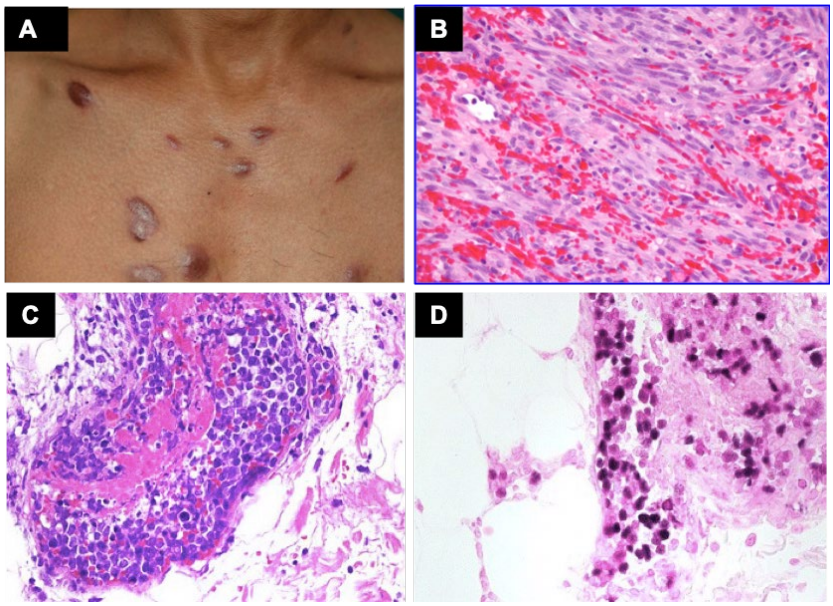

Fig. 1.2.2. KSHV and EBV are the etiological agent of human cancers. In immunocompromised host, KSHV oncogenicity results in Kaposi sarcoma which manifest as a raised skin lesion (A) and is an AIDS- associated cancer(Bhatia et al. 2017). The presence of spindle cells and abnormal erythrocyte extravasation to lesion (B) are dominant phenotypes of KSHV pathogenesis(E. Mesri, Cesarman, and Boshoff 2010). EBV resides in the memory and the antibody-producing B-cell compartment of healthy individuals but lack of immunosurveillance permits the expression of oncogenes that drive proliferation and acquisition of hyperplastic malignant phenotypes. EBV in-situ hybridization of small RNAs can be detected within tumors (C-D)(Cesarman et al. 2019a).

Primary effusion lymphomas (PEL), while caused by KSHV, 90% of cases are co-infected with EBV. A recent study in humanized mice found dual infection of KSHV and EBV develop tumors with PEL transcription signature, and tumorigenesis

was dependent on EBV lytic reactivation. Similarly, EBV lytic gene expression is elevated in patient-derived EBV and KSHV (McHugh et al. 2017). KSHV has been linked to the B Cell lymphoproliferative disorders of multicentric Castleman's diseases (MCD), which can progress to non-Hodgkin's lymphoma in some cases (Oksenhendler et al. 2002). The highly-proliferative plasmablastic lymphomas where KSHV induces overproduction of interleukin-6 (**Figure 1.2.2**).

1.2.2. Kaposi' Sarcoma

KSHV is the causative agent of the skin cancer of endothelial origin, it is composed of proliferating spindle-shaped cells, high infiltration, and concentration of inflammatory cells and cytokines, in addition to, the local formation of abnormal blood vessels (E. Mesri, Cesarman, and Boshoff 2010). The KS spindle cells express signature cellular markers at a different stage of tumorigenic progress like smooth muscle alpha-actin, desmin, and vimentin. The expression of vGPCR drives tumorigenesis and is a lytic-associated gene which subverts cellular pathways leading to the expression and secretion of angiogenic, pro-inflammatory and proliferative factors that act on the pro-oncogenic natural environment of latently infected cells. Therefore,

the lytic and latent replicative programs of KSHV are co-factors for sarcomagenesis (**Figure 1.2.2**).

1.3. Brief description of models to study the pathogenesis of human gammaherpesviruses

Given the strictness of host tropism of gammaherpesvirus, infection of laboratory mice by EBV and KSHV is very limited and poorly reflects the microorganism pathogenicity in a physiological state. Many experimental studies on viral-induced tumorigenesis make the use of cell lines derived from tumor lesions or lymphomas(McHugh et al. 2017; Mutlu et al. 2007; Myoung and Ganem 2011a; Sarosiek et al. 2010). In the case of KS-isolated cells, the continuous passage of results in the loss of KSHV episomal. Nonetheless, KSHV reinsertion with recombinant antibiotic-resistance genomes and ectopic expression of the lytic switch factor have represented an enriched model to study KS-KSHV biology and test efficiency of targeted therapies. KS spindle cells express signature cellular markers at a different stage of tumorigenic progress like smooth muscle alpha-actin, desmin, and vimentin(E. Mesri, Cesarman, and Boshoff 2010). In a seminal study, transfection of mouse bone marrow pro-angiogenic endothelial-lineage cells with a significant contrast containing the KSHV genome in a bacterial artificial chromosome (KSHVBAC36) was able to induce an angiogenic

phenotype similar of KS spindle cells while expressing latent and lytic KSHV genes in nude mice (Mutlu et al. 2007). These results indicate that KSHV infection collaborates with in vivo growth conditions provided by the host. The transcriptome of the virus-differentiated cell designated mEC36 clustered in between endothelial progenitors and mature vascular endothelial cells. Moreover, the same study demonstrated the role of the early lytic gene vGPCR plays in KS tumorigenesis (Mutlu et al. 2007). The same research team explored a xenograft model of PEL model B-lymphomas obtained from an elderly man during a pleural effusion tap in immunodeficient NOD/SCID mice immediately after tap. These mice developed peritoneal effusion, and solid lymphomas on the peritoneum and PEL cells maintained KSHV infection in vivo(Sarosiek et al. 2010). Both studies revealed differences in host and virus transcription in vivo versus in vitro.

The reconstitution of laboratory mice with human cells presents another valuable model. In a recent study, humanized NSG mice demonstrated that KSHV persists more frequently in the presence of EBV and enhances tumor formation. Dually-infected cells expressed hallmarks of PEL-like lymphomas with differentiation plasmablasts-like B-cells(McHugh et al. 2017).

1.3.1. Gammaherpesvirus infection of a natural host

Gammaherpesviruses can infect the animal kingdom, from bats to our closest primate relatives, the bonobos, and the chimpanzees. The closest phylogenetic relative available of KSHV is the rhesus monkey rhadinovirus (RRV) and Retroperitoneal fibromatosis herpesvirus (RFHV). EBV's closest relative is the rhesus monkey lymphocryptovirus (rhLCV)endemic in old world monkeys and widely studied. Large regions of both γHV genomes share conserved ORF position, and most contained at least one gene homolog suggesting similar selection pressures for the evolution in primates(Damania 2007). All capable of immortalizing B-cells in vitro. Naïve rhesus macaques orally infected with rhLCV develop typical EBV clinical manifestations of mononucleosis with an increase in activated-cytotoxic lymphocytes the first few weeks of infection consistent with a high viral load which declines to almost undetectable levels after 3-months post-infection [7] (**Figure 1.3.1**).

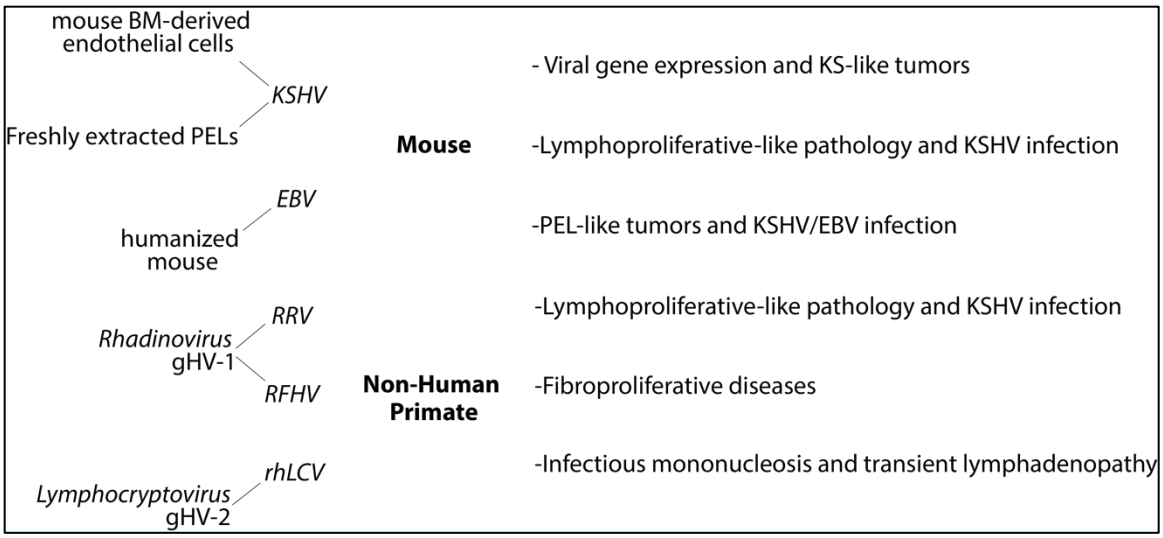

Fig. 1.3.1. Summary of animal models for human gammaherpesviruses pathogenesis. The use of laboratory animals has helped in understanding the mechanism in which infection of these viruses leads to oncogenesis. Irradiated SCID/NOD mice were employed for mEC36-KS model and PEL xenografts, which are impaired development of in T-, B- and NK-cells. Athymic nude mice for subcutaneous mECK36 cells implantation. NSG mice were reconstituted with human immune cells for KSHV and EBV dual infection experiment.

In experimental settings, infection of immunocompetent rhesus macaques with an RRV strain results in similar hyperplastic B cell lymphoproliferative manifestation, as seen in KSHV. However, this was resolved after 12 weeks-post infection, even after SIVmac239 co-infection reflecting the role of the immune system against viral replication (Mansfield 1999). Following death from immunosuppression induced by SIV infection, several monkeys revealed an arteriopathy histologically similar to the vascular endothelial lesions in KS. Notably, R1 (K1), vIL-6, vGPCR, RTA, LANA, and the polycistronic spliced transcript R8 and R8.1 (K8 and K8.1) carry similar molecular and biological

functions to their KSHV homolog. Beneficially, RRV carries a temporal transcription program during lytic infection similar to KSHV and can be grown lytically to high titers in rhesus fibroblasts, which offers an alternative model to the in vitro latent-restricted nature of KSHV. Moreover, the retroperitoneal fibromatosis-associated herpes virus (RFHV) was isolated from a colony of rhesus macaques affected with a vascular fibroproliferative disease that resembles KS (Rose 1997). A longitudinal-comprehensive study that spanned 15 years found a potential role for naturally acquired γHVs in the development of malignancies of SIV-infected rhesus monkeys. The data showed the presence of one or more γHVs in tumors with high DNA viral surrounding tissues. The pathology of these tumors recapitulated many features of malignancies that arise in HIV-infected individuals. Rhesus LCV was positive in diffuse large B-cell lymphomas; in a Burkitt-like lymphoma, RRV was predominant; and in fibrosarcoma, RFHV (Vickie Marshall 2018).

The Herpesvirus saimiri (HVS) is a rhadinovirus closely to KSHV and endemic in squirrel monkeys. While the genome organization and DNA sequence of HVS is highly similar to KSHV does not cause tumorigenesis even in immunosuppressive condition but highly pathogenic in primate species. HVS infects T-lymphocytes and is often used as a mechanism to

immortalize T-lineage cells(Fickenscher and Fleckenstein 2001). HVS has retained viral genes required for episomal maintenance of the genome, similar to LANA and, viral replication with homology to RTA. However, the signature immunomodulatory mechanism like vIL6 and vIRFs found in EBV and KSHV are absent in the HVS genome elucidating its divergence (Damania 2007).

1.3.2. Murine gammaherpesvirus-68 (MHV68)

Officially murid herpesvirus type 4 (MuHV-4) by the ICTV, the murine gammaherpesvirus isolate 68 (MHV68) was isolated from the bank vole species, *Clethrionomys glareolus* in Slovakia during an ecological canvassing for arboviruses in the forest of Eurasia. MHV68 is endemic to *Apodemus sylvaticus*, commonly known as wood mice, but can infect a wide range of rodents, belonging to diverse, phylogenetically distant families (Cipková-Jarčušková et al. 2013). Initially, an intracranial passage from mouse to mouse classified MuHV-4 isolates as alphaherpesviruses since it infected neurons, much like herpesvirus simplex. Later, analysis of the viral genome would reveal MuHV-4 is closely related to EBV and herpesvirus saimiri (Efstathiou et al. 1990; Efstathiou, Ho, and Minson 1990) but classified under the genus Rhadinovirus given the inability to immortalize B-cells as seen with KSHV.

The genome of MHV68 consists of 118 kbp of unique DNA flanked by variable numbers of 1.23 kbp terminal repeats (TR) regions (Nash et al. 2001). It contains 73 ORFs, the majority collinear, and homologous to those of the other gammaherpesviruses (Nash et al. 2001). The non-homologous or unique genes in the MHV68 genome are located in the same regions of unique genes in the KSHV and EBV genome (Song et al. 2005). However, viral genes involved in latency and reactivation of gammaherpesviruses are well-conserved between primate and rodent rhadinoviruses, in addition to large regions of the genome encoding proteins essential for virus replication.

A study published in the Journal of Virology compared infection outcomes of the commonly used laboratory mouse strain BALB/c with the natural host *A. sylvaticus*. Infection of the natural host yielded 3 log units lower of virus titers than BALB/c in the lungs, a site of virus expansion, and replication after intranasal infection (Hughes et al. 2010). In BALB/c mice, virus replication occurred in alveolar epithelial cells accompanied by a diffuse, T-cell dominated interstitial pneumonitis. On the other hand, replication in wood mice is restricted to the site of immune-cell infiltration containing macrophages that expressed viral antigen and, to a lesser degree, T cells (Hughes et al. 2010).

Latently infected lymphocytes were abundant in inducible bronchus-associated lymphoid tissue 14 days post-infection of wood mice but not apparent in laboratory mice. The establishment of latency in the spleens of infected wood mice was more rapid, with well-delineated follicle formation in germinal centers and significantly higher latently infected splenocytes. In strike contrast, BALB/c mice initially display a poorly defined germinal center. Moreover, MHV68 specific antibody titers were similar in both mice; however, the neutralization capacity was higher in antibodies from wood mice. The differences in infection outcome observed in the study reveal a better evolutionary adaptation by a natural host species resulting in an effective immune response. Nonetheless, MHV68 has proven to be an exceptional animal model revealing many fundamental core aspects of gammaherpesvirus pathogenesis and define immune responses under persistent infection(E. Barton, Mandal, and Speck 2011; Doherty et al. 2001).

Intranasal and intraperitoneal inoculation are the most common route for MHV68 infection of laboratory mice. While sexual transmission of MHV68 between laboratory mice (François et al. 2013) has been observed, it is generally believed that gammaherpesviruses it is naturally transmitted through saliva like other rhadinoviruses. This study found

genital excretion sites in female mice following intranasal infection and observed efficient virus transmission to naïve males after sexual contact (François et al. 2013).

Upon intranasal inoculation, a manifestation of a gammaherpesvirus acute infection ensues production of virions, interstitial pneumonitis, and clinical manifestations similar to those of EBV infectious mononucleosis. In the lungs, MHV68 viral titers expand at the expense of alveolar epithelial cells and macrophages which support lytic infection (**Figure 1.3.2**). Early studies also identified on-going lytic infection by in-situ viral RNA hybridization, within peribronchial and perivascular cellular infiltrates and be extended to draining-lymph nodes (E. Barton, Mandal, and Speck 2011; Sunil-Chandra et al. 1992). The expansion of virus titers during the lytic phase contracts within 10-12 days due to the rise of inflammatory effector cells and virus-specific cytolytic CD8 T-cells (Doherty et al. 2001).

Fig. 1.3.2. Course of MHV68 infection in laboratory mice. Upon intranasal inoculation MHV68 undergoes expansion by lytic replication. Local infection of B cells and antigen-presenting cells is believed to spread infection to distal lymph nodes and the spleen. As acute infection wanes, establishment of latency in the spleen initiates and is characterized by a transient expansion of CD4+ and CD8+ T cells and B cells. A viral-driven proliferation and differentiation of naïve, germinal center and isotype-switch B cells can be observed in the spleen at day 16 through day 18. During this period, 1 in 100 splenocytes harbor the virus latently while the virus' genetic program is switched to latency, and very few viral proteins are been expressed. Around 10% of latently infected

splenocytes undergo spontaneous reactivation and can be assessed by an infectivity assay when splenocytes are explanted to a cell layer permissive to MHV68 reactivation. Two months after the initial infection, MHV68 is harbored latently in 1 out of every 10,000 splenocytes, mainly plasma B cells. Unlike KSHV, MHV68 viral particles proceed to a default lytic replication in vitro in fibroblast and epithelial cells.

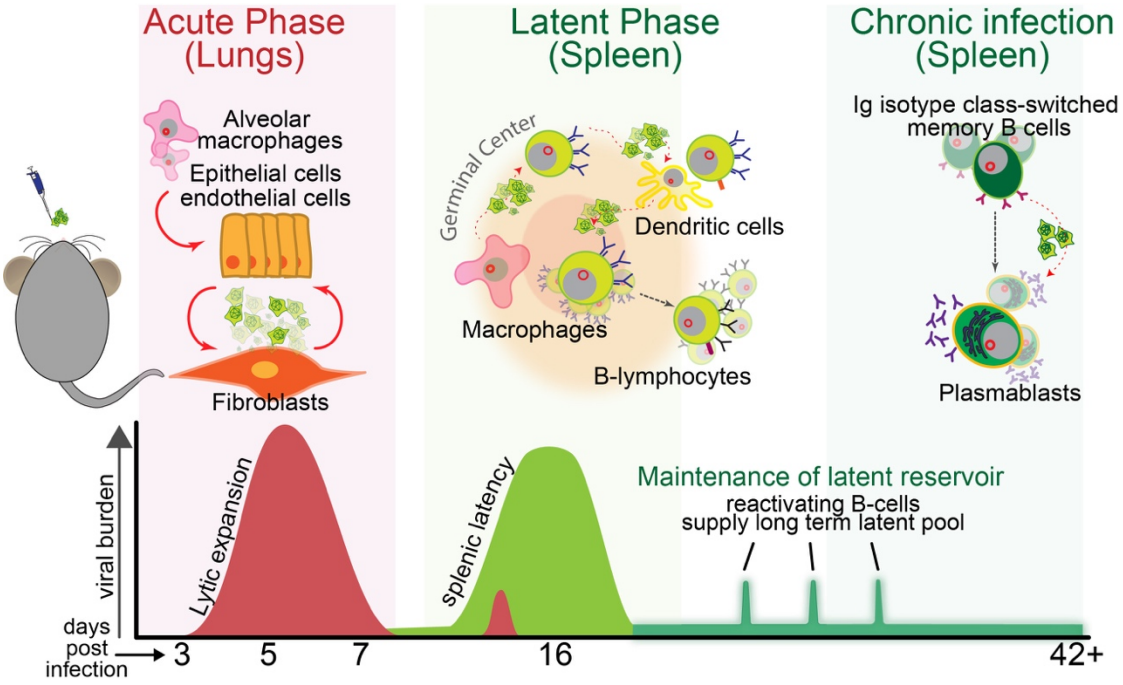

As acute infection wanes, MHV68 enters draining-lymph nodes and the spleen via infection of the macrophage-rich zone in the marginal sinuses. This splenic latency is predominated by B cell infection predominates. At this time, hematological manifestations comparable to EBV's mononucleosis can be observed within the spleen. Lymphadenopathy and splenomegaly are evident due to B-cell infection, their expansion, and the abundant numbers T-cells

responding to the lytic antigens produced during replication. Here, the cytolytic CD8 T-cells controlling the acute phase in the lung contract virus infection in the spleen 14 to 18 days post-inoculation. CD8 T-cell response is crucial to latency establishment since depletion results in a persistent lethal infection (Nash et al. 2001). A CD8 T-cell subset containing Vβ4TCR is the most abundant population in the spleen at this point of infection. The role of these cells remains elusive since their expansion is independent of the presentation by classical MHC class I or MHC class II molecules (E. Barton, Mandal, and Speck 2011). The activity of the CD4 T-cell compartment control early and long-term infection by production of IFN-gamma (shown to repress ORF50) and dendritic cell licensing, which enables prolonged activation of CD8 T-cell (E. Barton, Mandal, and Speck 2011) (**Figure 1.3.2**).

The marginal zone macrophages and follicular dendritic cells grant cell-entry to the B-cell compartment, not before incoming virions are released by epithelial cells. B-cells are, therefore, permissive only to myeloid-derived virions, which then infect the expanding population of the germinal center. Detection by fluorescent-tagging of the MHV68 genome has shown a high percentage of infection occurring in centrocytes and centroblasts, reaching immunoglobin isotype-

switched memory B cells, one of the primary reservoir of MHV68 latency (Collins et al. 2012). At this point, the frequency of MHV68 infection is roughly 1 in 100 splenocytes. The limiting-dilution assay, along with sensitive nested-PCR has allowed the field to determine a more accurate ratio of the frequency of cells carrying the MHV68 genome and capable of reactivating into a lytic replication (E. Barton, Mandal, and Speck 2011).

Two months after the initial infection, 1 out of every 10,000 splenocytes, mainly plasma B cells harbor the MHV68 genome (Flaño et al. 2002). Terminal differentiation to antibody-producing B-cells induces lytic reactivation and is believed to be driven by the very host-transcription factors that promote maturation to plasma B cells (A. M. Siegel et al. 2010). In addition, a latency-associated MHV68 product promotes B-cell differentiation into a plasma cell-like phenotype (Liang et al. 2011) while the exact mechanism of maintenance of long-term latency is unknown, the homeostasis of the immune compartment influences chronic infection (**Figure 1.3.2**).

A recombinant MHV68 carrying KSHV's G protein-coupled receptor replacing its murine equivalent induces angiogenic and inflammatory features of KS tumors in infected mice. Unlike KSHV, MHV68 viral particles proceed to a default lytic

replication in vitro in fibroblast and epithelial cells. Recently, it was shown that MHV68 could promote a persistent infection of lung endothelial cells in vitro and in vivo, by the continuous secretion of virions (Suárez and van Dyk 2008). MHV68 like KSHV establishes latency in the memory B cell compartment, providing a small animal model to study latent infection and reactivation of gammaherpesvirus, and the interplay of the host in their pathogenesis.

1.4. The interplay between the hypoxia-inducible factor 1 pathway and gammaherpesviruses

The term normoxia refers to the average oxygen concentration in the local tissue of an organism that maintains normal cell and tissue function. In addition, immune cells and hematopoietic stem cells transit through locations that vary local oxygen percentage.

The oxygen trail explains the different oxygen concentrations throughout the cells, tissue, and organs of an animal. Any disruption to oxygen delivery be it by stroke, injury or infection, that limits oxygen supply to organs, is quickly sensed by multiple molecular and cellular pathways. One of them is the hypoxia-inducible factor 1 (HIF1).

1.4.1. The HIF1 pathway: regulation and function

HIF1 was first described for its capacity to bind hypoxia-responsive elements (HRE or HREs for multiple) in the promoter region of genes involved in oxygen delivery (erythropoietin) and angiogenesis (angiopoietin). HIF1 is a transcription factor comprised of a heterodimer complex: HIF1-alpha (HIF1α) and the HIF1-beta (HIF1β) subunit. The DNA-binding motif of HIF recognizes the hypoxic response elements (HRE) with the consensus sequence 5′- RCGTG- 3′ in the promoter region of target genes. The HIF1 transcription complex binds the transactivators CPB and p300 that drives response to support cellular and tissue functions through the transcription of over eighty genes involved in a myriad of process oxygen deliver, angiogenesis, and ATP production through glycolysis ensuring cell survival. Dysregulation of the HIF1 function resulting in constitutive activation can lead to the expression of angiogenic growth factors and provide an excess of anaerobic metabolism supporting tumor formation.

Normoxia regulates the stability of the HIF1α subunit. Oxygen availability dictates hydroxylation of proline residues in HIF1α by prolyl-hydroxy dioxygenases (PHD) that causes a structural change, which is recognized by the Von

Hippel Lindau (VHL) tumor suppressor protein. Elongin B, Elongin C, and Cul2 associated with hydroxy- HIF1α and pVHL to form a ubiquitin-ligase complex that ubiquitinates HIF1α and prompts degradation via the 26S-proteasome complex, making HIF1α short-lived (5-15 minutes) (Greer et al. 2012). HIF1α is also regulated by hydroxylation of asparagine residue at the C-terminal. The Factor Inhibiting HIF1 (FIH) stops HIF1 transcriptional transactivity by blocking its interaction with CBP/p300. If HIF1α is not degraded. Inhibition of PHDs and FIH by the lack of oxygen, HIF1α accumulation translocates to the nucleus, where it partners with HIF1βand other transcription transactivators. Additionally, local deregulation of co-factors like ferrous-iron, and alpha-ketoglutarate (TCA cycle intermediate) affects PHD activity and stabilize HIF1α (**Figure 1.4.1**).

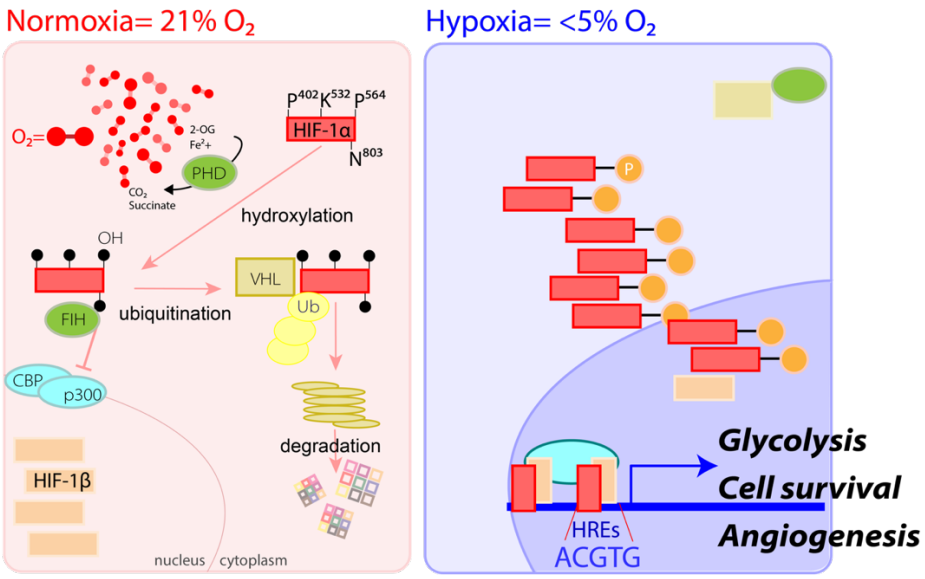

Fig. 1.4.1. Regulation of HIF1α. Oxygen is the main limiting factor for prolyl-hydroxylase dioxygenase (PHD) activity. The oxygen-dependent domain in HIF1α exposes proline residues which are hydroxylated by PHDs. The structural changes in hydroxy-HIF1α facilitates binding of VHL-ubiquitination complex which promotes proteasome-dependent degradation. Local oxygen depletion inhibits PHD function and HIF1α is stabilized. Accumulation leads to nuclear translocation for the transactivation of over eighty genes involved in oxygen homeostasis.

1.4.2. Gammaherpesviruses hijack the hypoxia-inducible factor 1 pathway

Current evidence shows that by employing several viral proteins, human gammaherpesviruses disrupt the molecular interactions that regulate HIF1α stability in the presence of oxygen. AIDS-KS tumor biopsies strongly stained for HIF1α in comparison to healthy tissues and co-stains with LANA in immunofluorescent assays. Substantial data demonstrates that several viral products directly binding HIF1α and can target HIF1α negative regulators. HIF1α also regulates the activity of many viral promoters, which contain hypoxia-responsive sequence homologs. One study identified four HRE cluster regions that bound HIF1α protein to viral promoter regions critical in lytic gene silencing, latency maintenance, and lytic reactivation by interacting with host transcription co-activators and host chromatin remodelers.

Hydroxylation by PHDs destines HIF1α for destruction. The stable expression of the 12 microRNAs in the KSHV microRNA cluster, downregulates the PHD2 gene, EGLN2, an isoform of

HIF prolyl hydroxylases and HIF1α antagonist (Yogev et al. 2014). Similarly, EBV stabilizes HIF1α in many transformed B-cell and epithelial cell lines. In lymphoblastoid-hybrid cells, PHD2 and PHD1 are sequestered by the latency-associated nuclear antigens EBNA-3 and EBNA-5, respectively, blocking catalytic activity (Darekar et al. 2012). The latent membrane protein 1 (LMP1) stabilizes and induces expression of Siah1 in nasopharyngeal epithelial cells, which blocks VHL interaction with HIF1 by targeting PHD1 and PHD3 for degradation (Kondo et al. 2006).

Hydroxy-HIF1α is recognized by the Von Hippel Lindau (VHL) complex and ubiquitylated by the Elongin BC/Cul2/pVHL ubiquitin-ligase complex, thereby marking HIF1α for degradation by the 26S proteasome. Biallelic inactivation of VHL in the renal adrenal carcinoma cell line 786-O has profound stabilizing effects on HIF1α protein levels resulting in high transcription activity. B-cell lymphomas have significantly reduced levels of VHL protein. The laboratory of Erle Robertson has shown that the latency-associated nuclear antigen (LANA) in KSHV inhibits HIF1α degradation by acting as a component of the cellular protein degradation pathway, Elongin BC/Cul2 ubiquitin complex. In a study, the authors characterized a SOCS-motif (suppressor of

cytokine signaling box-like-motif) in LANA, which interacts with the complex, submitting VHL to polyubiquitination and degradation. LANA exhibits increased stability when co-expressed with Elongin B and Elongin C, and the SOCS-box-like motif in LANA is a requirement for this stability. The same group has also shown that the high levels of HIF1α expression observed in infected B-cell lymphoma cell lines such as PEL could be explained by the capacity of LANA to bind the oxygen-dependent degradation domain of HIF1α, evading its degradation and leading to its accumulation. The silencing of LANA by siRNA in these cells significantly abrogated nuclear accumulation and the stabilization of HIF1α.

Another KSHV product, associated with the lytic program that strongly binds HIF1α, is the vIRF-3 (viral IFN Regulatory Factor 3)(Shin et al. 2008). The authors show results that suggest vIRF-3 binds and stabilizes newly synthesized HIF1α, transporting it to the nucleus. Immunofluorescence experiments show endogenous HIF1α co-localize with overexpressed vIRF-3 in SLK. Overexpression of vIRF-3 stabilizes HIF1α in the presence of Cycloheximide, an inhibitor of protein synthesis. In this study, each functional domain of HIF1α (bHLH, PAS, ODD, or TAD) was fused with GST (Glutathione S-transferase) to determine where does

vIRF-3 bind. The pull-down assay showed vIRF-3 binds to its DNA-binding motif and a lesser extent to the transactivation domain (TAD)(Shin et al. 2008).

Phosphorylation of HIF1α can modulate protein stability, subcellular localization, and transactivation (Kietzmann, Mennerich, and Dimova 2016). Gammaherpesviruses activate multiple signaling cascades transduction during infection, and this is necessary for virus-induced HIF1α accumulation. The angiogenic chemokine homolog in KSHV, vGPCR, induces members of the serine/threonine protein kinases family, MAPK (p42/44), p38alpha, and p38gamma and phosphorylates the HIF1α regulatory/ inhibitory domain (HID) (Sodhi et al. 2000). The same group later showed that vGPCR paracrine secretions upregulate HIF1α by activation of the mammalian target of rapamycin (mTOR)(Jham et al. 2011). HIF transcription activity was essential for secretion pro-angiogenic cytokines that promote tumorigenesis.

Similarly, the EBV-membrane protein, LMP1, is necessary for the accumulation of HIF1α protein in type II EBV latency epithelial tumor cells(Wakisaka et al. 2004). The same group claimed that this was dependent on the activation of the p42/44 MAPK pathway, in addition to the production of reactive oxygen species in a nasopharyngeal epithelial tumor cell

line. Chemical inhibitors were effective in decreasing HIF1α (Wakisaka et al. 2004). The ROS (Reactive Oxygen Species) scavenging agent N-acetyl-cysteine blocked HIF1α accumulation in cultured cells from constitutively active RAC1 tumor model, a downstream (Q. Ma et al. 2009). Constitutive signaling of vGPCR recruits the activity of the small signaling G-protein, Rac1 to the NADPH oxidase pathway leading to ROS production. It is of consistent opinion among the field that ROS-mediated production of inflammatory mediators, indirectly modify HIF1α via MAPK, ERK and PI3/AKT pathways regulating and enhancing its transactivation (Movafagh, Crook, and Vo 2015). Gammaherpesviruses can mediate the regulation of HIF1α transcriptional activity by ROS production.

While evidence for the stabilization of HIF1α is evident, a study revealed the capacity of ORF34, an HRE-containing lytic promoter, to bind HIF1α in vitro and induce its degradation via the proteasome pathway (Haque and Kousoulas 2013). Here, expression vector systems demonstrated the interaction of HIF1α (NH2-terminal bHLH and PAS domain only) with the ORF34 products (most robust interaction with COOH-terminal). The authors argue that ORF34 could compete with the potent HIF1α stabilizer, LANA, for HIF1α-binding

which control the lytic versus the latent status of KSHV infection (Haque and Kousoulas 2013)

1.4.3. Metabolic reprogramming by gammaherpesviruses is dependent on HIF1α induction

Much like cancer cells, KSHV infection induces the Warburg effect by shifting cells towards aerobic glycolysis while reducing oxygen consumption. Latently infected blood and lymphatic endothelial cells show high production of lactate and reduction in cellular oxygen consumption clear signs of metabolic reprogramming (Delgado et al. 2010a; Yogev et al. 2014). B-lymphoma derived cancer cell lines, BCBL-1, and BC-3, also show a shift in metabolism towards glycolysis in comparison to primary B cells (Bhatt et al. 2012). Reprogramming is dependent on the constitutive expression of HIF1α, while genetic silencing affected the expression of GLUT1, PK-M2, LDHA, and PDK-1, and reconstitutes oxygen consumption (Shrestha et al. 2017). Similarly, glycolytic genes are upregulated, and EBV-infected lymphoblastoid cell lines (LCLs) secrete high levels of lactate when compared to activated B-cells that are uninfected. Interestingly, the same was not observed in fresh EBV-infected B-cells after 24 hpi suggesting metabolic adaptation through cell transformation (Darekar et al. 2012).

In the final step of glycolysis, PKM2 converts phosphoenolpyruvate into two pyruvate molecules and ADP into ATP. The glycolytic enzyme, isoform M2 of pyruvate kinase (PKM2), is a critical HIF effector in the maintenance of aerobic glycolysis in KSHV-infected cells (Luo and Semenza 2011). Here, conditioned-media from cells overexpressing the lytic-associated vGPCR gene was enough to upregulate PKM2 in mock cells and can reach neighboring cells in an autocrine and paracrine fashion (T. Ma et al. 2015a). Overexpression of vGPCR, in HEK 293T cells, increases glucose uptake to similar levels as HIF1α vector expression and doubles in HIF1α/vGPCR co-expression condition (Singh et al. 2018).

The induction of aerobic glycolysis by gammaherpesviruses has been associated with the survival and growth advantage of latently infected cells. When HIF1α-induced glycolysis was interrupted in PEL cells (BCLB-1 and BC-3) by shRNA HIF1α, slower cell proliferation, and the reduction of colony-forming abilities ensues (Shrestha et al. 2017). Also, the sole expression of the KSHV miRNA cluster granted metabolically reprogrammed lymphatic endothelial cells a growth advantage in anaerobic conditions (Yogev et al. 2014).

Disturbances to the energetic status quo of the host can disrupt latent infection. For instance, inhibitors of glycolysis were shown to selectively induce apoptosis in KSHV infected an endothelial cell in comparison to their uninfected counterpart (Delgado et al. 2010a). In another study, reversing aerobic glycolysis by induction of cellular respiration caused substantial expression of lytic genes and viral replication. Here, cell death was not caused by Resveratrol, which increases mitochondrial biogenesis, but by the activation of the lytic phase. These results suggest that a state of aerobic glycolysis is necessary for the maintenance of latency (Yogev et al. 2014).

1.4.4. HIF1α is necessary for the angiogenic phenotype in γHV-associated malignancies

HIF1α plays a significant role in vasculogenesis during embryonic development and angiogenesis, in utero, and adults. Following episodes of low oxygen such as in cases of ischemia or injury, sprouting-angiogenesis is initiated. The parenchymal cells of the ischemic, or affected tissue, upregulate HIF1α, which directly activates transcription of pro-angiogenic factors, most importantly, the vascular endothelial growth factor (VEGF). Once secreted binds the vascular endothelial growth factor receptor (VEGFR) in

neighbor cells prompting angiogenic budding of new capillaries from existing vessels.

The laboratory of Enrique Mesri was the first to identify HIF1α activation as a viral oncogene mechanism to hijack the host angiogenic pathways leading to KS (Bais et al. 1998; Sodhi et al. 2000). In the seminal study, vGPCR-induced angiogenesis through activation of the MEK/MAPK and MKK6/p38 pathways. The serine/threonine kinases phosphorylate TAD-HIF1α enhancing VEGF expression. Other viral genes, like vIL-6 and the viral-encoded chemokines, are expressed in a proportion of cells in KS lesions and possess tumorigenic activities that amplify the angiogenic phenotype (E. Mesri, Cesarman, and Boshoff 2010).

An evidence-supported hypothesis for KSHV-induced tumorigenesis is the exchange of paracrine- and autocrine-secreted factors between ~5% of lytically-infected cells and ~95% of latently-infected cells. These exchanges drive proliferation, angiogenesis, inflammation, and, finally, genetic instability (Cavallin et al. 2018; E. A. Mesri, Feitelson, and Munger 2014). Tumor allografts generated by injection of athymic nu/nu mice with the vGPCR-expressing endothelial cells (10% “lytic”) plus vCyclin/vFLIP-expressing cells (90% “latent”) treated with Digoxin, a HIF1α inhibitor,

develop smaller tumors and low expression of HIF1α and VEGF (Jham et al. 2011). Similarly, this group demonstrated increasing levels of pyruvate kinase-2 and HIF angiogenic genes like VEGF, ANGPT2, and ANGPLT4 in latently infected endothelial cells; however, sole expression of vGPCR provided tumorigenic potential in a PKM2-HIF1α dependent manner (T. Ma et al. 2015a). Finally, vIRF-3 stabilized HIF1α induces VEGF mRNA and secretion enough to prompt tube formation of HUVECs (Shin et al. 2008)

1.4.5. Gammaherpesviruses recruit HIF1α to the genome maintaining latency and regulating lytic replication

The presence of functional HREs within viral promoters and the recurrent interaction of HIF1α with the KSHV genome proposes a role for viral gene transcription. At least 16 viral promoters contain a relatively higher degree of the conserved HRE sequences, ACGTGC and GCGTGC, defined as hypoxia-responsive clusters within the KSHV genome. Seven of sixteen HRE-containing viral genes coincide with binding sites for the host transcription factor RBP-Jk (RBS) (Zhang et al. 2014b). The major downstream effector of the Notch signaling pathway RBP-Jk is responsive to hypoxic-stress and has proven to be essential in the maintenance of latency and lytic reactivation of KSHV (Scholz et al. 2013). Latency is

maintained by repressing the lytic expression of HRE/RBS-containing viral promoters by the HIF1α and RBP-Jk associated to the LANA-inhibitory-complex.

In vitro, KSHV infected cells are reactivated into a lytic replication by treatment with chemical compounds that target, directly and indirectly, transcriptional activation of RTA (Myoung and Ganem 2011b). In a similar manner, exposing infected cells to low oxygen conditions induce mRNA accumulation of RTA and other lytic genes such as the ORF34-37 cluster (Haque et al. 2006). LANA cooperates with HIF1α bind to HREs within the RTA promoter to directly induce lytic gene expression for lytic replication (Cai et al. 2006; Haque et al. 2006; Veeranna et al. 2012). However, many groups have found that HIF1α is stabilized and highly accumulated in PEL and KS cells in normoxia while maintaining a latent status. In instances, the N-terminal of LANA was found to associate with HIF1α in KSHV infected cells of B-lymphoma origin, BCBL-1 cells in co-IP, and IFA assays. A recent study shines a light on the matter by describing a post-translational modification in LANA (SUMOylation) that recruits hypoxia-sensitive chromatin remodelers like KAP1 and Sin3. The deletion of this motif results in a loss of the KSHV genome turns on lytic gene expression, and elimination of KAP1 by

siRNA enhances lytic gene expression in hypoxia. In low oxygen conditions, KAP1 and Sin3 dissociate from LANA, allowing interaction with RBP-Jk and HIF1α to drive RTA expression beginning the lytic reactivation cascade.

In normoxic conditions, the sole expression of LANA upregulates HIF1α mRNA through direct interaction with its promoter, suggesting a positive feedback loop (Veeranna et al. 2012). HIF1α can bind to LANA independently of HRE presence, suggesting prior recruitment. Hypoxia has been found to enhances the induction of KSHV lytic reactivation by chemical inducers (David A Davis et al. 2001). In this first study, the B-lymphoma cell lines, BC-3 and BCBL-1 were treatment with 12-)-tetradecanoylphorbol-13-acetate, or TPA for short at 21% O2 or 1% O2. After 72 hours, intracellular staining viral proteins showed a dramatic increase in the expression of the nuclear protein PF-8 and the viral envelope glycoprotein gpK8.1 at 1% O_2. They also showed the presence of a minor capsid protein (ORF 6) in supernatants belonging to cells treated TPA and incubated in low oxygen conditions for 96-hours. The same laboratory recently demonstrated that stable HIF1α knockout in PELs, reduced viral gene and protein expression of RTA, vIL-6, and the late lytic gene, ORF 26 (Shrestha et al. 2017).

EBV is also induced to lytic replication in low oxygen conditions. Initially, it was found that similarly to TPA treatment, hypoxia treatment induced the gene expression of the reactivation activator in EBV, BZLF1 in the marmoset B-cell line EBV-transformed, B95-8. In a luciferase reporter plasmid containing the BZLF1 promoter, hypoxia-induced transcription activation of the EBV lytic-associated gene while RT-qPCR revealed higher copy numbers of virus-specific region 48 hours post-hypoxia when compared to TPA alone (Jiang et al. 2006). Additionally, treatment with hypoxia-mimic Deferoxamine (DFO), increased expression of the lytic protein in EBV positive cell lines (Kraus et al. 2017). The authors revealed that HIF1α primarily induced EBV lytic-gene expression by activating transcription from the HRE sequences in the BZLF1. Interestingly, HIF1α did not activate the orthologue of RTA in KSHV, BRLF1, or Rta. Finally, they prove in a model for B-cell lymphoma induced by EBV in mice, that latently infected cells express lytic-associated antigens in vivo when located in a poorly oxygenated physiological environment. Moreover, exposure of latently infected mouse B-cell lymphomas with murine gammaherpesvirus (MHV68) to hypoxic conditions increased cell surface expression of lytic-associated antigens. Expression of HIF1α and HIF2α in

a vector system can activate transcription of the RTA promoter, which also contains HREs (Polcicova et al. 2008). Altogether, this indicates that besides the transcription factor function employed by these viruses in cellular modulation, the DNA-binding capacity in the HIF1α subunit regulates both latency and lytic replication in gammaherpesvirus pathogenesis. Given the vast array of functions in KSHV and EBV biology, HIF1α is an attractive therapeutic target to treat KSHV-positive lymphoma cells. Treatment of lymphoma cells with the HIF1α inhibitor, PX 478, affected proliferation rate by 72 hours in a dose-dependent manner when compared to two KSHV-negative Burkitt's lymphoma cell lines and latently infected Vero cells uninfected (Shrestha et al. 2017).

1.4.6. Hypoxia and KS

Accumulative data strongly suggests that HIF1 and low oxygen potentiate the pathogenesis of gammaherpesviruses. The sporadic induction of the lytic program, within tumors, could be triggered by HIF1α accumulation, whose downstream effector function synergizes with the latency program promoting cell transformation and development of a malignant phenotype. Tissue injury, in which blood vessels and capillaries are severed, disrupts oxygen delivery prompting a local hypoxic

response. High occurrence of KS lesions following surgical procedures developing within wounds and blood clots in KSHV-seropositive individuals could influence tumorigenesis. Coined, the Koebner phenomenon, it refers to the observation that patients with certain skin disorders, who develop new lesions in previously healthy skin succeeded by trauma. The new lesions are comparable to those in diseased skin (Maral 2000). In a case study, the authors described the development of KS in the scar site of biopsy, which had no previous pathologic abnormalities or KSHV expression (Webster-Cyriaque 2002). In correspondence to the authors, Dr. Yarchoan et al. suggested that hypoxia is the mechanism that promotes lesion formation. Besides the local inflammatory changes to the site of injury, which recruits circulating KSHV-infected cells such as macrophages, endothelial progenitors and B-lymphocytes, the hypoxic conditions occurring around the edges of the wound may activate latent KSHV into lytic gene expression conducive to paracrine oncogenesis (E. Mesri, Cesarman, and Boshoff 2010; Yarchoan, Davis, and Rinderknecht 2002).

CHAPTER 2

A ROLE OF THE HYPOXIA-INDUCIBLE FACTOR 1 ALPHA IN MOUSE GAMMAHERPESVIRUS 68 (MHV68) LYTIC REPLICATION AND REACTIVATION FROM LATENCY

2.1. MHV68 infection upregulates HIF1α expression and transcriptional activity

We first determined whether MHV68 upregulates HIF1α during virus infection in culture. The mouse fibroblast cell line NIH 3T12 was infected with a wild type MHV68 strain in normoxia (21% O_2), HIF1α mRNA and protein levels were analyzed by qRT-PCR and western blot, respectively. Figure 1 shows upregulation of HIF1α protein at early time-points during MHV68 infection, which increases over time. Cobalt chloride ($CoCl_2$), a hypoxia mimic was used as a positive control (Epstein et al. 2001). Accumulation of HIF1α protein correlated to a 6-fold increase in HIF1α mRNA levels (**Figure 2.1.1B**) at 24 hpi when compared to uninfected cells indicating that induction of HIF1α activity by MHV68 occurs together with activation of transcription. Moreover, transcription of HIF1α was dependent on viral gene expression, as we did not detect HIF1α mRNA upregulation when cells were exposed to UV-inactivated virus (**Figure 2.1.1B**). We next sought to determine whether upregulation of HIF1α during MHV68 infection activates HIF1α mediated transcription of host

HIF1-regulated genes, which containing HRE-binding sites at the regulatory region using an HRE-dependent luciferase reporter in a dual-luciferase assay.

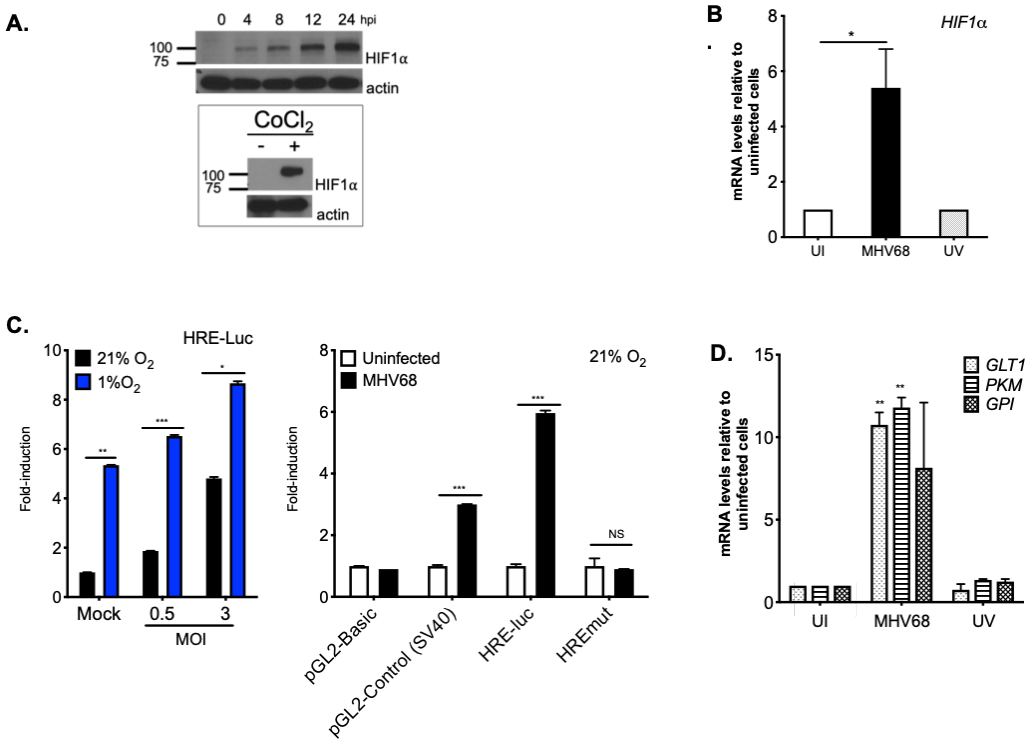

Fig. 2.1.1. MHV68 infection upregulates expression of HIF1α. (A) 3T12 fibroblasts were infected with a wild type strain of MHV68 (WUMS) (5 MOI) at 21% O_2 (cell culture incubator) and protein lysates were analyzed by western blot for the expression of HIF1α protein at different time-points. A second set of cells were treated for 8 hours with the hypoxia-mimic $CoCl_2$, which served as positive control (enclosed right panel). (B) HIF1α mRNA at 24 hpi expressed as fold-change in cells infected with MHV-68 or UV-irradiated virus relative to uninfected cells. Data shown is the average three independent experiments carried out in triplicates. Statistical analysis by Student's t-test, mean±SEM. *, $p<0.05$. (C) 3T12 cells were transiently transfected with pRL-TK (Renilla) and pGL2 vector which contains the three hypoxia response elements from the Pgk-1gene (Emerling et al. 2008) for 12 hours followed by MHV68 infection (MOI = 0.5 and 3.0). Cells were transferred to, 21% O_2 or normoxia (black bar) or 1% O_2 or hypoxia (blue bar) and HRE-driven luciferase activity was measured at 24 hpi (Left). The fold induction values are firefly/renilla units normalized to uninfected cells at 21% O_2. HRE-dependent responses (Right) by HREmut-Luc activity (24hpi, MHV68 MOI:3.0) are firefly/renilla units normalized to uninfected cells. Data shown in graph is the average of three experiments performed independently with triplicates. Statistical analysis by Multiple Student's t-test, mean ± SEM. *, $p<0.05$. **, $p<0.01$. ***, $p<0.005$ (D) mRNA levels of HIF1 alpha targeted host genes such as GLT1, PKM and GPI were measured by qPCR at 24 hpi. Uninfected and UV-

irradiated MHV68 virus were used as negative controls. GLT1= glucose transporter 1, PKM= pyruvate kinase, GPI= glucose-6- phosphate isomerase. Data shown in graph is the average of three experiments performed independently with triplicates. Statistical analysis by Multiple Student's t-test, mean ± SEM. **, $p<0.01$.

3T12 cells were transfected with reporter or control vectors and then infected under normoxia (21% O_2) and hypoxia (1%O_2) at different MOI. We found an increase in firefly luciferase reporter activity 24 hpi in cells infected with MHV68 in comparison to uninfected controls (**Figure 2.1.1C**) which was higher in hypoxia than normoxia suggesting that both infection and hypoxic conditions contribute to the enhancement of HIF1α transcription activity. Upregulation of HIF1α by oncogenic gammaherpesviruses is central to the induction of metabolic reprogramming which occurs via upregulation of HIF1α regulated genes such as glucose transporter 1 (GLUT-1), glucose-6 phosphate isomerase (GPI) and pyruvate kinase (PKM). These are key enzymes required for energy production during cellular adaptation to low oxygen supply. We, therefore, determined if HIF upregulation by MHV68 lead to an increase in transcription of these metabolic HIF-target genes using qRT-PCR. Transcription of genes was increased 7 to 5-fold in MHV68 infected cells (**Figure 2.1.1D**) and was dependent on virus infection as cells exposed to UV-irradiated virus failed to induce upregulation of HIF1α-

regulated genes. Taken together, the data depicted in this chapter shows that MHV68 infection upregulates HIF1α levels and transcriptional activity.

2.2. Genetic ablation of HIF1α DNA binding domain suppresses HRE-dependent transcription

Upregulation of HIF1α protein during MHV68 infection indicates that this transcription factor plays a role during virus replication. We, therefore, sought to evaluate the impact of HIF1α on lytic replication and viral expression in knock-out cells. We obtained primary MEFs from transgenic knock-in mouse (B6.129-Hif1α^{tm3Rsjo}/J), with exon 2 of the HIF1α gene flanked by 34bp specific LoxP sites (HIF1αLoxP MEFs) (Tang et al. 2004). Exon 2 encodes the DNA-binding region required for the dimerization of the protein in the nucleus and transcription of HIF1 target genes. A cre-recombinase expressing lentivirus was employed to transduce HIF1αLoxP MEFs followed by selection for resistance to the antibiotic Blasticidin. We first characterized both HIF1α wild-type (WT= MEFs from HIF1αLoxP transgenic mice) and HIF1α 1α Null cells (Null= HIF1α 1αLoxP MEFs expressing Cre-recombinase) by performing mRNA analysis with specific HIF1α oligonucleotides for HIF1α cDNA. Exon 2 deletion was detected as a fragment

size shift to 400bp in HIF1α Null cells in contrast to the complete 600bp PCR product spanning exon 1 to exon 5 in non-transduced HIF1αLoxP MEFs (**Figure 2.2.1A**). Also, no amplification of exon 2 was detected by qPCR in Null cells when compared to WT MEFs, and no change of expression was observed in Exon 4/5 transcripts (**Figure 2.2.1B**).

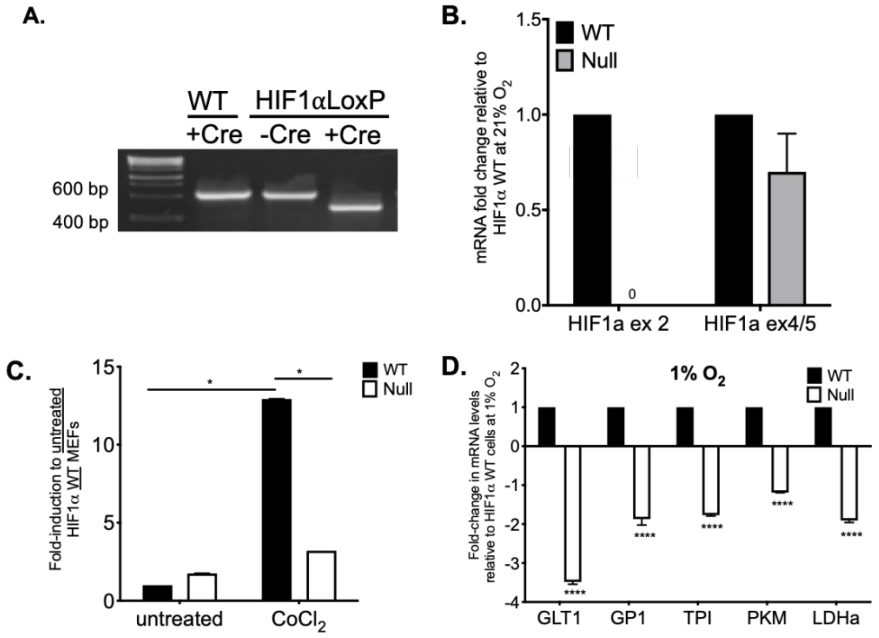

Fig. 2.2.1. Deletion of HIF1α DNA-binding domain suppresses HRE-dependent transcription in hypoxia. (A-D) Mouse embryonic fibroblasts (MEFs) were isolated from 13.5-day old embryo from B6.129-Hif1α^{tm3Rsjo}/J (HIF1αLoxP) and C57BL/6J (WT) and were immortalized by culturing cells over 30-35 generations. Immortalized HIF1αLoxP MEFs cells were transduced with a lentivirus vector expressing Cre-recombinase (Lenti-Cre) and selected with Blasticidin. MEFs (WT) isolated from parental mice was used as corresponding control for all experiments. (A) Excision of exon 2 was detected by amplification of gene fragment spanning exon 1 to exon 5 by PCR. A 400 bp fragment corresponds to the excised exon 2 in Null MEFs (+CRE) in comparison to 600 bp fragment (-CRE) in HIF1αLoxP MEFs. (B) HIF1α mRNA expression in WT and Null cells were measured by qPCR with primers from Exon 2 region. Exon 4/5 from HIF1α primer was used as corresponding control and was detected in both WT and Null cells. (C) WT and Null MEFs were either treatment with the hypoxic mimic cobalt chloride ($CoCl_2$) to induce HRE-driven luciferase expression for 8 hours or left untreated. Data shown in graph is the average of three experiments performed independently with triplicates. Statistical analysis by

Multiple Student's t-test, mean ± SEM. *, $p<0.05$. (D) WT and Null MEFs were exposed to 1% O_2 and HIF1 alpha target genes such as Glutamate transporter (GLT), Glucose-6-Phosphate Isomerase (GPI), Triose-phosphate Isomerase (TPI), Lactate Dehydrogenase A (LDHa), Pyruvate Kinase M1/2 (PKM) were measured by qPCR. ΔΔCt normalized against WT infection at 21% O_2 and displayed as $2^{-\Delta\Delta Ct}$ fold-change. Data shown in graph is the average of three experiments performed independently with triplicates. Statistical analysis by Multiple Student's t-test, mean ± SEM. ****, $p<0.0001$.

Null cells were further analyzed to confirm that they lacked HIF1α transcriptional activity using an HRE-luc reporter and qRT-PCR for HIF1α-regulated genes as done in **Figures 2.2.1C and D.** Luciferase signal was 10-fold less in Null cells following 8-hour treatment with the hypoxia mimic $CoCl_2$, indicating HIF1α dependent activity was impaired. Also, transcription of HIF1α-regulated glycolytic genes was also verified by qRT-PCR in Null cells. Each HIF1α transcript exhibited a significant decrease in expression after 8-hour treatment in 1% O_2 conditions, confirming that HIF1α protein was inactive in Null cells.

2.3. Absence of HIF1α activity impairs MHV68 replication *in vitro*

Next, we assessed whether the absence of HIF1α transcription activity could affect virus lytic replication. HIF1α wild-type (WT) and Null MEFs were infected with high and low MOI of MHV68 virus, viral supernatants were harvested at different times post-infection (dpi), and amount of

infectious virus was determined by plaque assay. Figure 2A shows HIF1α protein expression is downregulated in Null MEFs at 24 hours of infection. Comparing virus titers in WT and Null cells inoculated with varying MOI, virus production was decreased uniformly in the absence of HIF1α. As shown in Figure 2B, time-course infection of Null cells at 5.0 MOI showed a slight reduction while a lower infection of 0.5 MOI had a significant decreased in virus production at later time-points. These results suggest a role for HIF1α during lytic replication. Thus HIF1α is necessary for the efficient production of infectious particles during MHV68 replication.

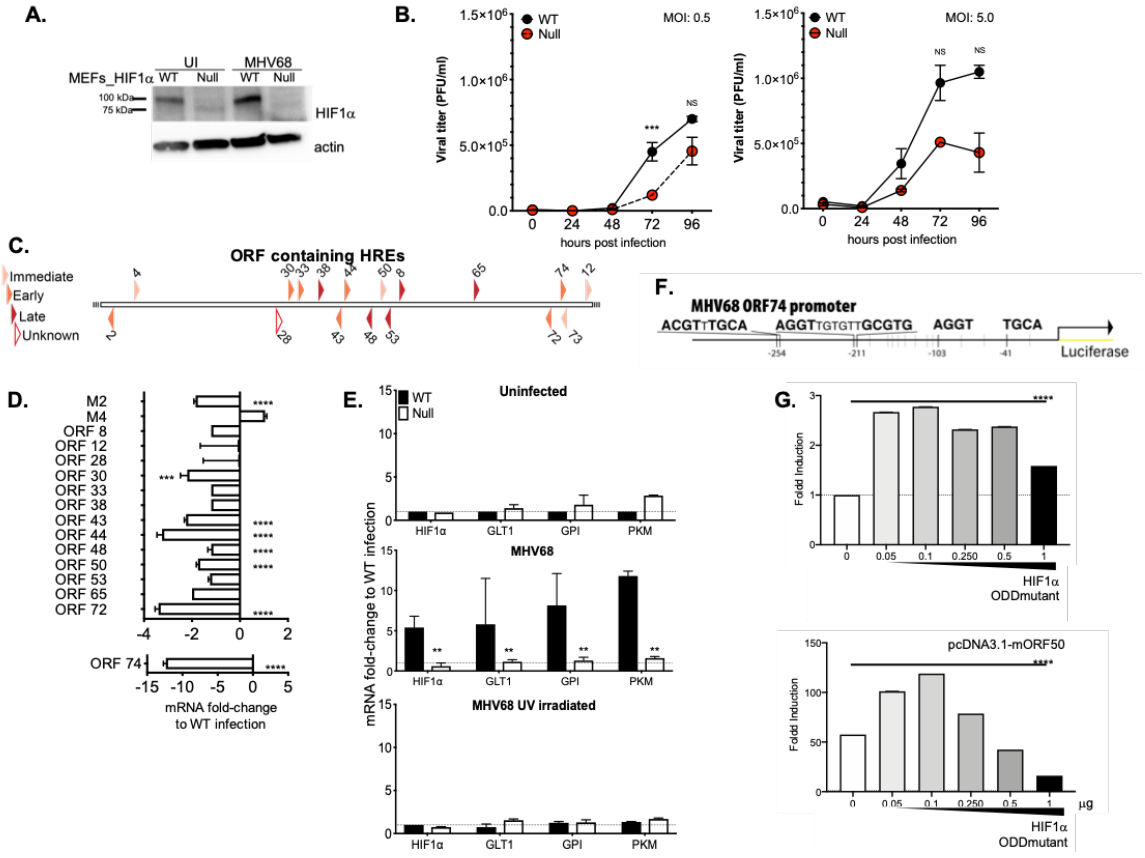

Fig. 2.3.1. Viral replication is compromised in the absence of HIF1α and is required for transcriptional activity of HRE-containing viral and host genes. (A) Stably transduced WT and Null MEFs were infected with wild type MHV68, WUMS strain at 5 MOI and HIF1α protein levels were measure 24 hpi (B) MHV68, WUMS strain at 5 MOI (Left) and 0.5 MOI (Right) in normoxia. Virus supernatants were collected at 0, 24, 48, 72 and 96 hpi and assayed for released virus by plaque assay on 3T12 cells. Data shown in graph is the average of three experiments performed independently with triplicates. Statistical significance was determined in Graph Pad Prism by multiple Student's t- test. ***, p< 0.005. NS abbreviates no statistical significance. (C) Schematic diagram of MHV68 open reading frame promoters containing 1 or 2 potential HIF1α binding sites (R-CGTG) was analyzed using TRANSFAC database. The diagram categorizes time of expression upon de novo lytic infection of MHV68 in 3T12. White polygon represents an unknown function. (D) WT and Null MEFs were infected with wild type MHV68 (MOI 5.0) and incubated at 21% O_2. RNA was isolated 24 hpi and changes in viral open reading frames (ORF) was measured by qPCR. ΔΔCt was expressed as fold change and normalized against WT MEFs infection. Data shown in graph is the average of three experiments performed independently with triplicates. Statistical significance determined by multiple t-test using the Holm-Sidak method, with alpha= 0.05. (E) WT and Null MEFs were infected with wild type MHV68 as in 4B. RNA was isolated 24 hpi and levels of mRNA for GLT1 (glucose transporter 1), PKM (pyruvate kinase) and GPI (glucose-6- phosphate isomerase) were determined by qPCR; ΔΔCt was expressed as fold change and normalized against uninfected HIF1α WT MEFs. Data shown in graph is the average of

three experiments performed independently with triplicates. Unpaired t-test with Welch's correction P< 0.01. (F) HRE sequences within MHV68 ORF74 gene promoter. (G) 293 cells were transiently transfected with 1) reporter containing MHV68 ORF74 promoter upstream of luciferase in pGL2-Basic vector, overnight. 2) increasing amounts of HIF1α mutant plasmid (see methods). 3) addition of pcDNA3.1-mORF50 (bottom) or pcDNA3.1 vector (top). Data shown is the mean±SEM of three experiments performed independently with triplicates. Multiple Student's T-test analysis. **** P< 0.001.

2.4. Absence of HIF1α impairs viral gene expression in MHV68

The murine gammaherpesvirus shares significant homology with human gammaherpesviruses such as KSHV and EBV and encodes for several viral orthologs. HIF1α transcriptionally upregulates KSHV genes containing the HRE consensus sites (5'-ACGTG-3') in hypoxia (Cai et al. 2006), and HIF1α regulates viral persistence by binding HRE homologs located throughout the genome (Zhang et al. 2014a). Thus, we analyzed MHV68 viral promoters containing the consensus HIF1α binding motif with the Biobase TRANSFAC database. The transcription element search system was employed to identify potential transcription binding sites containing the string site RCGTG within 500 base pairs upstream of the starting codon of all the MHV68 open reading frames. The results, depicted as a diagram in **Figure 2.3.1C**, predicted 17 viral promoters with HREs in all classes of MHV68 genes (immediate-early, early and late), including the KSHV orthologs of open reading frames (ORFs) 43, 44, 50 (RTA), 73 (LANA) and 74 (vGPCR) which belong to the hypoxia-responsive KSHV clusters (Zhang et al. 2014a).

A qRT-PCR was performed in infected WT and HIF1α Null cells to measure mRNA levels of these 17 MHV68-HRE containing and non-containing ORFs. Viral mRNA was harvested from infected cell lysates 24 hpi since cytolysis is low, and virus production is present. The absence of HIF1α activity decreased transcription of many HRE containing viral genes in Null cells when compared to the transcript levels of WT MEFs (Fig. 2D and Supplementary Table 1). Within the HRE-containing viral genes, the most notable downregulation was observed for the viral G protein-coupled receptor (vGPCR/ORF74), a KSHV viral gene known to regulate HIF1α transcriptional activity and angiogenesis in KS (Jham et al. 2011; T. Ma et al. 2015b; Singh et al. 2018). Also, viral cyclin D homolog (ORF72), and ORF73, latency-associated nuclear antigen (LANA) were reduced 3-fold Several HRE-containing viral genes designated for viral replication such as ORF44, a component of DNA helicase-primase complex and ORF65, a DNA packaging protein was downregulated 2-fold and was statistically significant. Taken together, our results indicate that HIF1α may directly or indirectly regulate expression of HREs-containing viral genes required for optimal growth kinetics during MHV68 replication.

2.5. HIF1α activity is required to induce host genes during MHV68 replication

MHV68 infection of 3T12 cells increased transcription of glycolytic genes (**Fig. 2.1.1D**). This data is in line with the observation that herpes virus infections induce glycolysis through the anabolic pathway in order to support increased demand on cellular translation machinery required during viral replication and also to maintain latently infected cells (Carroll et al. 2006).

We undertook the analysis of genes involved in glucose uptake after virus infection in WT and Null cells. UV-irradiated virus and mock-infected MEFs were used for negative controls. Lytic infection upregulated up to 5-10 folds several enzymes such as glucose transporter 1 (GLT1) which is involved in glucose uptake (Huang et al. 2012), glucose-6 phosphate isomerase (GPI), which is the first enzyme in glycolytic pathway, and pyruvate kinase (PKM), which catalyzes the final step of glycolysis (Fig. 2E). The increase in gene expression in WT MEFs was dependent on replication of the virus as the UV-inactivated virus did not induce aerobic glycolysis or HIF1α in WT MEFs. In contrast, glycolytic gene expression was consistently similar to uninfected in Null cells. (**Figure 2.3.1E**), suggesting that the transcriptional activity of HIF1α is required for the

induction of glycolytic enzymes during MHV68 lytic replication.

2.6. The vGPCR (mORF74) viral promoter of MHV68 contains hypoxia-responsive elements and is transcriptionally activated by HIF1α expression

Downregulation of ORF74 mRNA in HIF1α Null cells (**Figure 2.3.1D**) and the presence of HREs consensus (**Figure 2.3.1F,** ACGTG, AGGTG, GCGT) within this promoter point to a role for HIF1α in transcriptional regulation of the viral gene. In order to determine HIF1α dependent transcription activation, the promoter region spanning nucleotides at -597 to start codon of ORF74 was inserted upstream of the luciferase reporter pGL2-Basic vector. MHV68 ORF74 promoter luciferase construct was transiently transfected into 293AD cells with increasing amounts of an oxygen-degradation insensitive HIF1α mutant. **Figure 2.3.1G** (top) shows statistically significant 2.6-fold activation to mock transfection. Moreover, the addition of expression vector containing full-length MHV68 RTA (mORF50) further enhances promoter activity (2-fold) in the presence of constitutively active HIF1α (**Figure 2.3.1G**-bottom). These findings suggest a role for transcription regulation of MHV68 ORF74 by HIF1α, as previously observed in KSHV vGPCR (Singh et al. 2018).

2.7. siRNA silencing and drug-mediated inhibition of HIF1α impairs MHV68 replication

In order to rule out any confounding effects due to the long-term impact of HIF1α exon 2 deletion in Null cells, we carried out two alternative approaches to inhibit HIF1 activity during MHV68 lytic infection. First, 3T12 cells were transfected with a HIF1α siRNA for 24 hours, followed by infection in normoxic conditions. The top panel of Figure 3A confirms HIF1α protein expression is abolished in HIF1α siRNA cells of uninfected and MHV68 infected cells cultured at 3% O_2. Silencing of HIF1α during normoxic infection significantly reduces viral titers by 20-fold at 48 hpi, on average, and drastically downregulates the expression of lytic replication genes (**Figure 2.7.1A**– 2nd row).

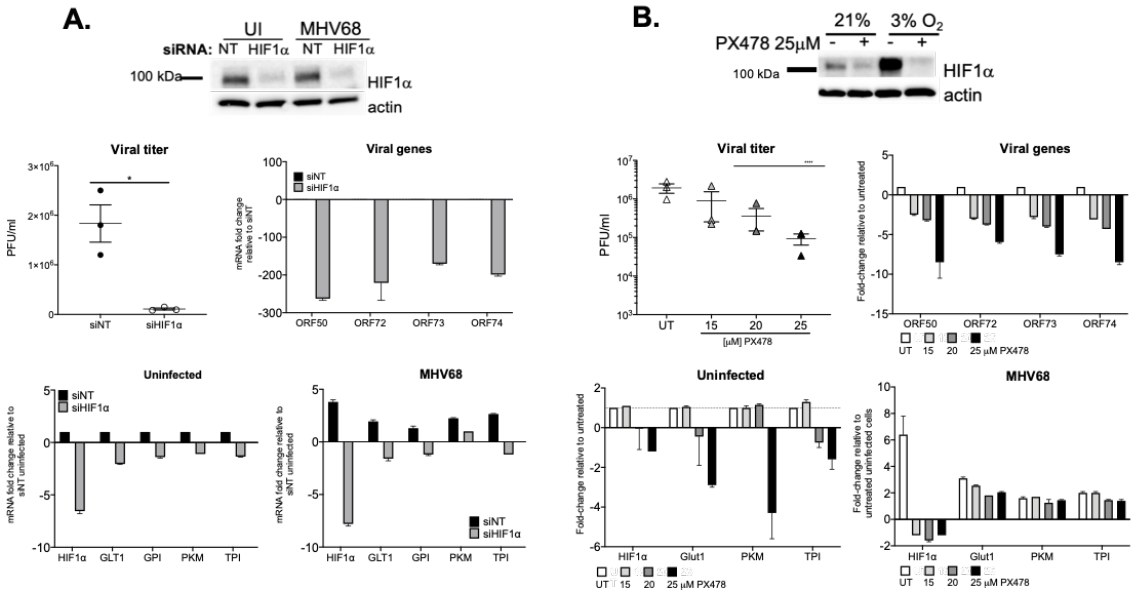

Fig. 2.7.1. Alternative approach to deplete HIF1α impairs MHV68 replication. (A) 3T12 cells were treated with a pool of siHIF1α or siNT

(non-targeting) for 24 hours. Top panel: HIF1α protein expression at 24hpi of uninfected and MHV68 (MOI:3) infected cells at 3%O_2. Beta-actin was probed for loading control. Middle panel: Plaque assay and RT-qPCR determine amount of virus released in supernatant at 48pi and fold-reduction in mRNA levels of RTA (ORF50), vCyclin (ORF72), LANA (ORF53) and vGPCR (ORF74) at 24hpi of siHIF1α-infected cells, respectively. (B) 3T12 cells were inoculated with MHV68 (MOI:3) then treated with various concentrations of the HIF1α inhibitor, PX-478. Top panel: HIF1α protein expression at 24hpi in 21% O_2 and 3%O_2. Middle panel: Plaque assay and RT-qPCR determine amount of virus released in supernatant at 48pi and fold-reduction in mRNA levels of RTA (ORF50), vCyclin (ORF72), LANA (ORF53) and vGPCR (ORF74) at 24hpi of untreated and PX-478 treated cell, respectively. (A-B) Bottom panel: RT-qPCR determine fold-changes in the mRNA levels of HIF1 alpha targeted host genes such as GLT1, PKM, GPI, TPI and HIF1α. Fold change is determined using $2^{(-\Delta\Delta Ct)}$ and ΔΔCt is the subtraction of Ct values from uninfected and MHV68-infected cells, untreated and HIF1α depleted cells as it stated in y-axis title. GLT1= glucose transporter 1, PKM= pyruvate kinase, GPI= glucose-6- phosphate isomerase, TPI= Triose-phosphate Isomerase. Data shown in graphs are average of three experiments performed independently with triplicates. Statistical significance determined by multiple t-test using the Holm-Sidak method, with alpha= 0.05.

In the second approach (**Figure. 2.7.1B**), we utilized PX-478, a small molecule inhibitor that has been shown to potently inhibit HIF1α transcription activity (Koh et al. 2008), in addition to reducing HIF1α protein and mRNA synthesis (Shrestha et al. 2017). In the first row of Figure 3B, we show 3T12 cells exposed to 25μM of PX-478 decrease in HIF1α expression 24hpi, even HIF1α-induced conditions. After MHV68 incubation, infected 3T12 cells were treated with 15, 20, and 25μM of PX478 and cultured at 21% O_2. At 48 hours, viral titers in supernatants from 25 μM PX478 were 10-fold less than titers from untreated supernatants. Moreover, the extent of the downregulation of lytic genes, 24 hours prior, was parallel with the increment in PX-478 concentration

(**Figure 2.7.1B**- 2nd row). Finally, blocking HIF1α activity through these approaches also impaired MHV68-induced expression of glycolytic genes (**Figure 2.7.1B**- 3rd row). These data confirm our observations, pointing to a critical role for HIF1α in MHV68 lytic replication.

2.8. HIF1α is necessary for optimal MHV68 replication in lower, physiological, oxygen levels

Our data demonstrate that the absence of HIF1α affects viral gene expression and virion production during lytic replication in normoxia. However, oxygen levels may play a profound role during in vivo infection as tissues and organs are usually characterized by their unique oxygenation status. During low oxygen availability, HIF1α accumulates binding to promoter regions carrying specific HRE elements. Therefore, we speculated that lower oxygen levels along with the effects in lack of HIF1α will be more profound.

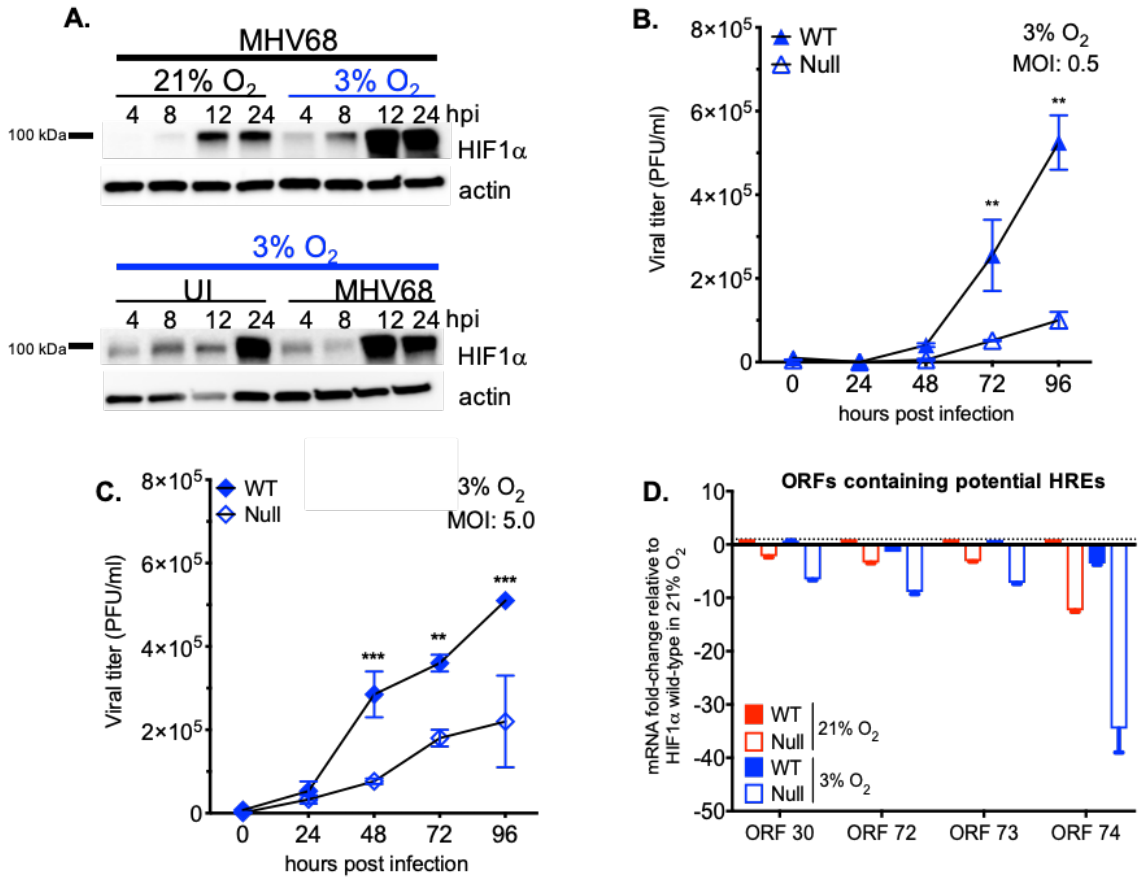

Fig. 2.8.1. Absence of HIF1α impairs gammaherpesvirus lytic replication in low oxygen concentration. (A) HIF1α expression during MHV68 time-course infection at 3% O_2 (4,8,12 and 24 hpi) was measured by western blot. (B) HIF1α WT and HIF1α Null MEFs were infected with MHV68 (B: MOI 5.0) in a single-step and (C: MOI 0.5) in a multi-step infection and transferred to 3% oxygen. Released virus in the supernatant was measured by plaque assay. Graph represents one of at least three independently performed experiments with similar results. Statistical significance was determined in Graph Pad Prism by Student's t- test with n=3. **, P< 0.01; ***, P< 0.005. (D) Selected viral genes with statistical significance p<0.05 of HIF1α Null 3% O_2 normalized to HIF1α Null 21% O_2.

Gene name	Possible function	Fold-change		
		21% O_2	3% O_2	
		HIF1α Null	HIF1α WT	HIF1α Null
M2	IL-10 driven B cell proliferation and differentiation	-1.9	-1.3	-4.6
M4	Complement regulatory protein	1.1	1.4	-1.7
ORF 8	Glycoprotein B	-1.2	1.9	-1.3
ORF 12	Encodes potential Zinc-binding motif	-1.2	1.4	0.9
ORF 28	Unknown	-1.1	1.9	-0.3
ORF 30	Unknown	-2.2	-1.4	-6.6
ORF 33	Unknown	-1.2	1.7	-1.4
ORF 38	Viral tegument protein	-1.2	1.8	-1.3
ORF 43	DNA packaging protein; minor capsid protein; UL6	-2.2	1.0	-4.1
ORF 44	Component of DNA helicase-primase complex	-3.4	1.0	-7.0
ORF 48	Unknown	-1.3	1.3	-1.8
ORF 50	Reactivation and transcriptional activator	-1.8	-1.4	-3.6
ORF 53	Unknown	-1.3	2.3	1.0
ORF 65	DNA packaging protein	-2.0	2.1	-1.7
ORF 72	Cyclin D homolog	-3.4	-1.4	-8.9
ORF 73	Latency Associated Nuclear Antigen	-3.2	0.9	-7.2
ORF 74	vGPCR (IL-8 receptor homolog)	-12.4	-3.6	-34.6

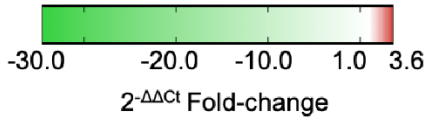

Fig. 2.8.2. Absence of HIF1α impairs gammaherpesvirus gene in low oxygen levels. HIF1α WT and HIF1α Null MEFs were infected with MHV68 (MOI 5.0) and transferred to either 21% and 3% oxygen, RNA was isolated 24 hpi. Levels of mRNA for MHV68 ORFs with HRE were determined by qPCR; ΔΔCt normalized against WT infection at 21% O_2 and displayed as $2^{-\Delta\Delta Ct}$ fold-change. Heat map was created using GraphPad Prism. Statistical significance displayed as asterisk (*, $p<0.05$) were determined using GraphPad Prism by Bonferroni's multiple-comparison test as following: column 1: 21% O_2 HIF1α Null vs 21% O_2 HIF1α WT, column 2: 21% O_2 HIF1α WT vs 3% O_2 HIF1α WT, column 3: HIF1α Null vs 21% O_2 HIF1α WT.

We performed a western blot analysis to determine the expression of HIF1α protein after virus infection in 3% O_2 conditions hypoxia since physiological levels of oxygen in many tissues ranges 3-7% (Nathan and Singer 1999b). 3T12 cells were infected with wild type, MHV68 in normoxia for 2 hours in 21% O_2 and then moved to a hypoxia chamber. Cell lysates were harvested 4-24hpi, and HIF1α expression was analyzed by

western blot analysis. In **Figure 2.8.1A**, we show that low levels of O_2 enhanced the accumulation of HIF1α protein during virus infection.

The role of HIF1α on MHV68 replication at different oxygen levels was assessed in WT and Null MEFs infected with high and low MOI of the virus by quantifying virion production at various times. **Figure 2.8.1B** demonstrates that viral expansion in the absence of HIF1α decreases especially as low MOI infection progresses under low oxygen tension with 2.3 and 4.5-fold change at 72 and 96 hpi, respectively.

To understand how oxygen level may affect the ability of HIF1α to regulate viral gene expression during virus infection, transcription analysis of HRE containing viral genes was performed 24 hpi as in **Figure 2.8.1D** and **2.8.2**. The data is represented by relative fold-change values, which were normalized against infected WT and Null MEFs under normoxic conditions (**Figure 2.8.2**). Absence of HIF1α at low oxygen levels had a 10-fold reduction in expression of several HRE-containing genes such as cyclin D, LANA, and vGPCR. This decrease was most notable in some HRE containing viral genes including vGPCR, which was reduced 34.6-fold in Null cells when compared to WT MEFs under 3% oxygen. Non-HRE viral genes, including ORF9 and ORF25, were also strongly downregulated at

3% O_2 in the absence of HIF1α (**Figure 2.8.1C** and **Figure 2.8.2**). Mainly, viral proteins related to viral and DNA replication (ORF9, RTA), assembly and latency associated genes such as LANA (ORF73), cyclin D (ORF72) and M2 (**Figure 2.8.2**) were impacted by low oxygen level conditions in Null cells.

2.9. The role of HIF1α in MHV68 *in vivo* pathogenesis

Our data showed that HIF1α protein plays a significant role in the replication of MHV68. However, it is unknown the exact role that the HIF1α pathway plays in gammaherpesvirus pathogenesis. Since infection of mice with MHV68 provides a tractable animal model that manifests the fundamental strategies for gammaherpesvirus pathogenesis (E. Barton, Mandal, and Speck 2011), we took advantage of genetic ablation of HIF1α in the $HIF1\alpha^{LoxP/LoxP}$ mice by infection (**Figure 2.9.1A**) with a recombinant MHV68 virus encoding the Cre-recombinase protein under CMV promoter (MHV68-Cre) (Moser et al. 2005). Homozygous deletion of HIF1α is lethal for development through embryogenesis (Semenza 1999), we utilized Cre-LoxP strategy to generate HIF1α deletion during MHV68-Cre infection. Several studies have reported the use of engineered MHV68 encoding Cre-recombinase gene to study virus-host interaction (Dutia et al. 2009; Reese et al. 2014; Stevenson et al. 2010). Our objective was to achieve deletion

of exon 2 in HIF1α locus in tissues by infection with a MHV68-Cre virus.

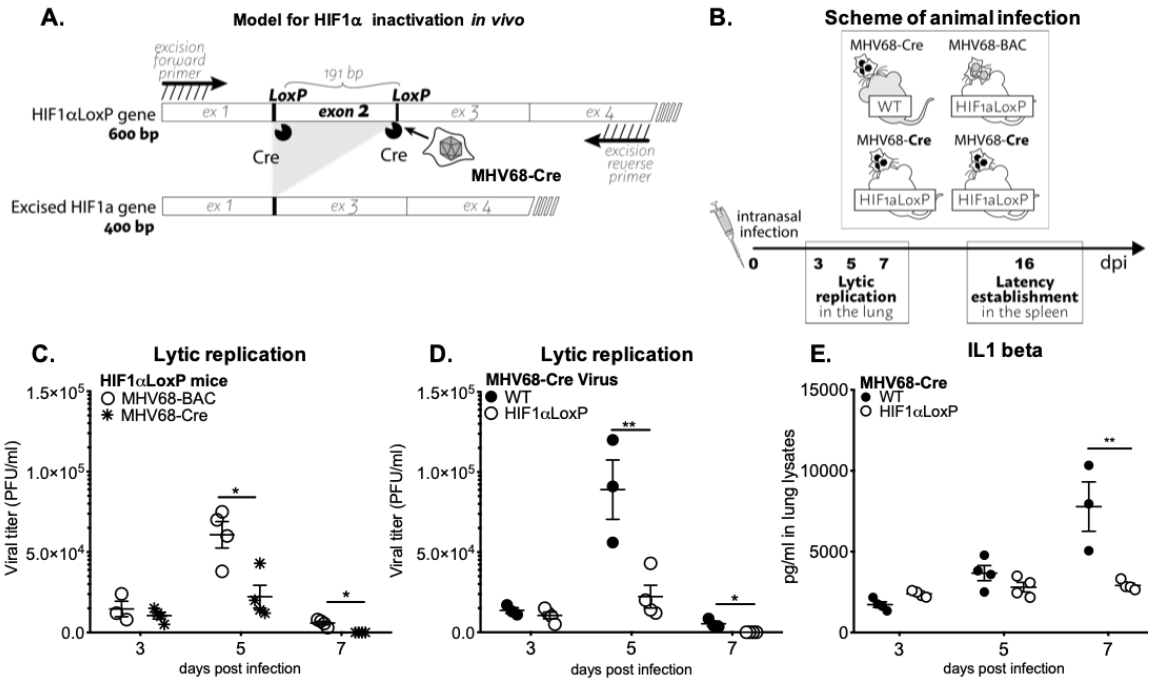

Fig. 2.9.1. HIF1α deletion affects *in vivo* virus growth expansion during acute infection. (A) Diagrams depict HIF1α inactivation by MHV68-Cre virus infected cells. (B) Scheme of animal infection. (C-D) C57BL/6J (WT/B6) mice (n=3-4) or B6.129-Hif1α^{tm3Rsjo}/J (HIF1αLoxP /B6) mice (n=3-4) were infected with MHV68-Cre virus by intranasal infection. Viral replication was measured from whole lung homogenates at 3, 5- and 7-days infection by plaque assay. Viral plaques were counted 5 dpi and expressed as PFU/ml. HIF1αLoxP mice were infected either with wild type MHV68 virus, (C) BAC-derived (n=3-4) or (D) MHV68-Cre virus (n=3-4) and lungs were assayed for viral titers as in 5A. Virus replication was significantly decreased on day 5 ($P<0.012$) or day 7 ($P<0.0016$). (E) Both WT and HIF1αLoxP mice were infected with MHV68-Cre virus and lungs were collected as described in 5A. ELISA was performed from lung homogenates to measure IL1 beta, TNF alpha, IL6 and IFN gamma. There were no differences in cytokine production between the two mice background, except for the marked decrease in IL-1beta from lungs of HIF1αLoxP mice on day 7 ($p=0.12808$) in comparison to WT. Graph represent one experiment (n= 3-4 mice) of three independent experiments, with similar viral titer differences. Statistical analysis was performed in Graph Pad Prism by Multiple Student's-t-test.

MHV68 undergoes a period of lytic replicative expansion in the respiratory tract and to a lesser extent in the spleen after intranasal infection of laboratory mice. Robust viral

replication in the lungs is characterized by infectious virion production and is cleared within 10-15 dpi (E. Barton, Mandal, and Speck 2011). In order to define whether HIF1α plays a role during MHV68 infection, we examined virus replication in lungs and latent virus establishment and reactivation from splenocytes. C57BL/6 WT (wild-type) and HIF1$\alpha^{LoxP/LoxP}$ mice were infected intranasally with 3 X 10^4 PFU of MHV68-Cre (**Figure 2.9.1B**) virus. A second set of experiments were performed in HIF1$\alpha^{LoxP/LoxP}$ mice infected with MHV68-BAC (parental strain for the recombinant virus) to validate that transgenic mice equally supports MHV68 replication (**Figure 2.9.1B**).

Lungs were harvested on days 3, 5 and 7 post-infection and viral titers were measured from lung homogenates. MHV68-Cre virus established infection in both WT (1.3 X 10^4 PFU/ml ± 1.8 X 10^3) and HIF1$\alpha^{LoxP/LoxP}$ mice (7.1 X 10^3 PFU/ml ± 2.4 X 10^3) by day 3 post-infection (**Figure 2.9.1C**). However, there was a 4-fold reduction of virus titer (2.2 X 10^4 PFU/ml ± 7 X 10^3) in HIF1$\alpha^{LoxP/LoxP}$ mice on 5 dpi when compared virus titers in C57BL/6 WT (8.9 X 10^4 PFU/ml ± 1.9 X 10^4) mice. The decline in viral titers continued until day 7 post-infection with titer below the limit of detection for HIF1αLoxP infection when compared to 5.4 X 10^3 PFU/ml ± 1.6 X 10^3 virus in WT mice

(**Figure 2.9.1C**). The decrease in acute viral replication was related specifically to deletion of HIF1α activity, as viral kinetics and production were not affected in HIF1α$^{LoxP/LoxP}$ mice infected with MHV68-BAC (wild type) virus (**Figure 2.9.1C**). The mean PFU/ml was 1.5 X 10^4 PFU/ml ± 4.8 X 10^3 on 3 dpi, and 6.0 X 10^4 PFU/ml ± 8.2 X 10^3 on 5 dpi in these mice (Figure 2.9.1C) and was similar to viral titers observed in WT (C57Bl/6J) mice infected with MHV68-Cre virus.

Early innate immune responses to MHV68 infection is accompanied by inflammation (Bortz et al. 2018; Hughes et al. 2010; S R Sarawar et al. 1996; Sally R. Sarawar et al. 2002). Inflammatory cytokines involved in this process, include interleukin-1 beta (IL1β), and TNFα. Several cytokines such as IL1β, IFNβ, IL-6, TNFα and IFNγ were analyzed from lung homogenates by ELISA from WT and HIF1α$^{LoxP/LoxP}$ mice infected with MHV68-Cre virus. Although there was a trend in reduction of cytokine production in lungs from infected HIF1α$^{LoxP/LoxP}$ mice on day 7 when compared to C57Bl/6 mice, the levels were not statistically significant (data not shown) except for IL1β which was reduced 3.5-fold in floxed mice (**Figure 2.9.1E**). The reduction in proinflammatory cytokines on day 7 post-infection in the absence of HIF1α activity may be due to early viral clearance reflected titers at day 5. We conclude

that inhibition of HIF1α activity during acute MHV68 infection impairs virus expansion in the initial days of infection.

Similar to human gammaherpesviruses, following virus clearance in the lungs, MHV68 establishes life-long latency in the host (Nash et al. 2001; Sunil-Chandra et al. 1992), and the spleen is the primary site of the latent reservoir. The establishment of latency is observed as early as day 16 post infection, where a substantial number of splenocytes (mostly naïve B cells) can be reactivated to produce lytic virus when co-cultured in vitro with permissive cells (Weck et al. 1996, 1999).

Fig. 2.9.2. Excision of HIF1α decreases viral reactivation from latency in infected splenocytes in vivo. C57BL/6J mice (n=3-4) or B6.129-Hif1α^{tm3Rsjo}/J (n=3-4) were infected with MHV68-Cre virus by intranasal infection. Splenocytes were harvested on day 16. (A) Limiting-dilution PCR was performed from infected WT and HIF1αLoxP splenocytes with two rounds of PCR were performed against MHV68 ORF50. There were no statistical differences (P=0.4350) between the two groups of mice infected with MHV68-Cre virus. Data represent results for one experiment (n=5 for each mice strain) out of two experiments (B) Ex vivo reactivation by limiting-dilution assay was performed to determine the frequency of infected WT and HIF1αLoxP splenocytes that harbor the viral genome. The frequency of cells reactivating the virus in HIF1αLoxP mice were less (1 in 73,181 splenocytes), when compared to C57Bl/6J mice (1 in 16,818 splenocytes) and was statistically significant (P= 0.0287). For both limiting-dilution assays, curve fit lines were derived from nonlinear regression analysis. Symbols represent the mean (n=5 per mice strain) percentage of wells positive for virus CPE +/- the standard error of the mean. (The dotted line represents 63.2%, from which the frequency of cells reactivating virus was calculated based on the Poisson distribution. Data represents results of one experiment (n=5 per mice strain) out of more than three independent experiments. Statistical significance was determined in Graph Pad Prism by Student's t- test. *, p< 0.05. (C) RNA from 10^7 splenocytes (25ng per PCR rxn) of WT and HIF1αLoxP mice were analyzed for excision of HIF1α exon 2 by PCR and the products were run on DNA agarose gels. Tissue from an uninfected naïve HIF1αLoxP mouse was

used as negative control. A 400bp fragment was observed only HIF1αLoxp and not in parental WT mice when infected with MHV68-Cre virus.

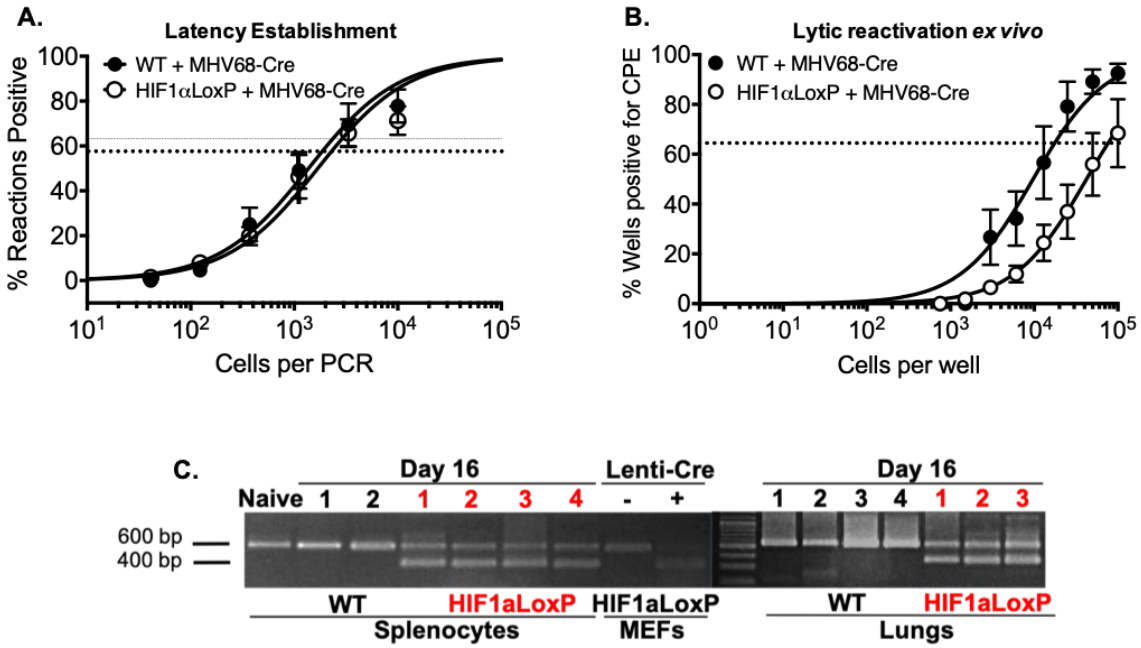

Therefore, we determined whether HIF1α plays a role during viral latency establishment in vivo and reactivation ex vivo. C57BL/6 (WT) and HIF1α$^{LoxP/LoxP}$ mice were infected with MHV68-Cre virus and splenocytes were harvested on days 16. The frequency of splenocytes harboring viral DNA (establishment) was determined by nested PCR. This assay has single-copy sensitivity for ORF50, which equates to one viral genome-positive cell. On the y-axis, the percentage of reaction positive for viral DNA against each cell dilution on x-axis. There were no significant differences in latency establishment in infected HIF1α$^{LoxP/LoxP}$ (1 in 2,880 cells) and WT mice (1 in 2,346 cells) on 16 dpi (**Figure 2.9.2A**). The

same splenocytes were assayed to measure the frequency of reactivating virus by ex vivo limiting dilution assay (LDA). Splenocytes were diluted 10-fold and co-cultured with primary MEFs for two weeks. The number for the frequency of cells reactivating was determined based on the Poisson distribution which predicts that 0.1 PFU per well should result at 63% percent reactivation of wells positive for cytopathic effect (CPE) (Moser et al. 2005).

In contrast to latency establishment, significantly fewer splenocytes reactivated in HIF1αLoxP (1 in 73,181 splenocytes) mice when compared to WT infection (1 in 16,818, P= 0.0287) upon ex vivo culture as shown in **Figure 2.9.2B**. We also confirmed that the transgenic background did not affect the frequency of viral reactivation by LDA assay from splenocytes harvested from HIF1α$^{LoxP/LoxP}$ mice infected with wild type (MHV69-BAC) virus. We validated the excision of exon 2 in vivo on RNA isolated from lung tissue and bulk splenocytes on16 dpi. A 400 bp PCR product corresponding to the excised HIF1α gene was observed only in the lungs and splenocytes of HIF1α$^{LoxP/LoxP}$ mice infected with MHV68-Cre virus (**Figure 2.9.2C**). A 600 bp product relating to full-length HIF1α gene in uninfected (naïve) or in WT mice infected with

the same virus confirmed that cre-recombinase was functional in vivo.

2.10. *Ex vivo* reactivation of MHV68-infected splenocytes in hypoxia enhances virus production

MHV68 lytic reactivation was negatively affected by Cre-virus-mediated inactivation of HIF1α, suggesting that it plays a role during the latent to lytic switch *ex vivo* in normoxic conditions. This is consistent with our results in Figure 2.3, which show that HIF1 deletion impairs de novo lytic replication. However, the impact of HIF1 activation during viral reactivation of γHV-infected cells derived from a natural host has not been explored.

Since low oxygen levels stabilize and activate HIF1, we sought to assess whether these conditions could affect the frequency of reactivation in MHV68-infected cells. Following latency establishment of a wild-type MHV68 infection in vivo, we carried out a limiting-dilution assay under 3% O_2 or 21% O_2 culture conditions, as performed in **Figure 2.10.1**. There was no significant difference in the average frequency of reactivating splenocytes cultured in both oxygen levels (21% O_2: 1 in 42,743 cells and 3% O_2: 1 in 29,498 cells), as shown in **Figure 2.10.1A**. This indicates that HIF1 activation by low oxygen conditions does not affect the rate at which cells reactivate into lytic replication in MHV68-infected cells.

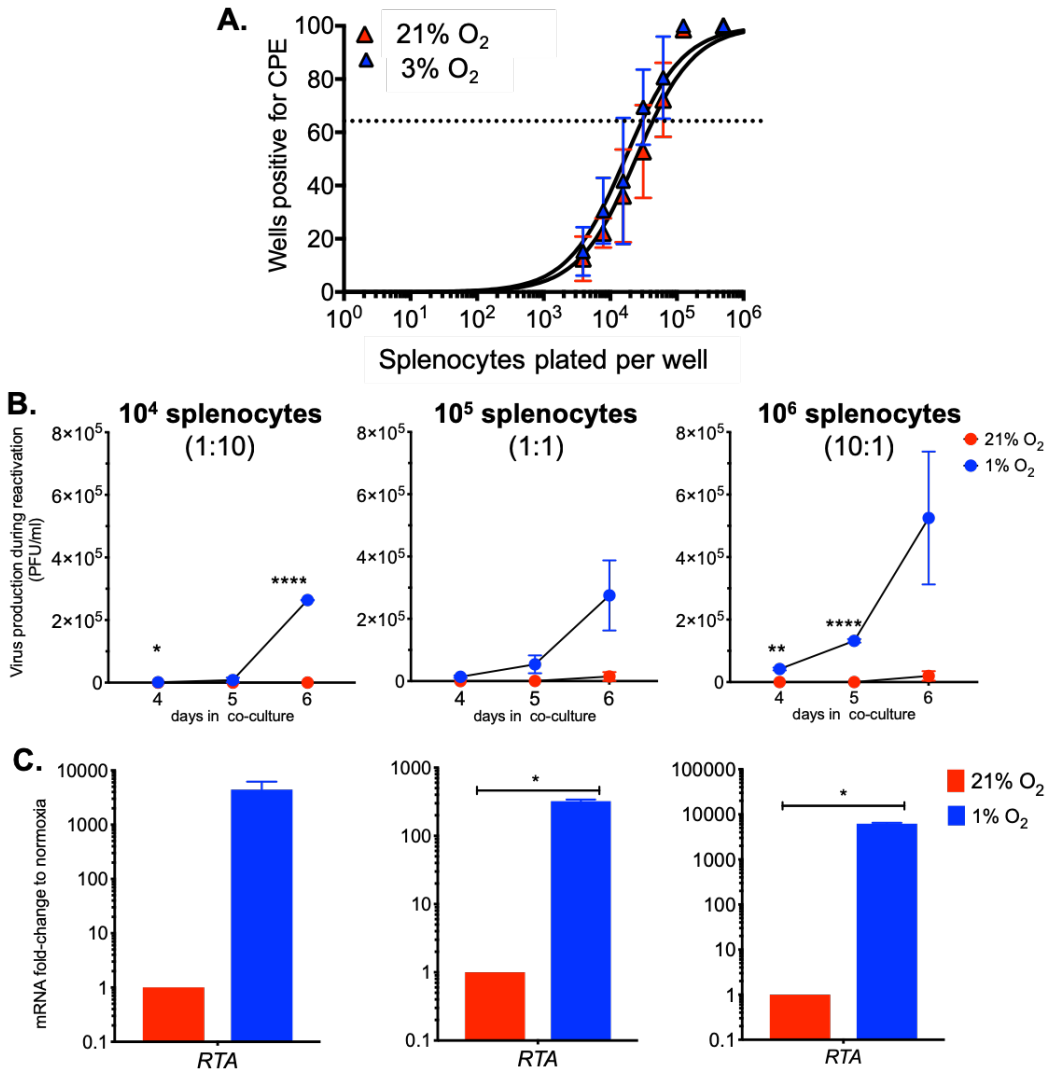

Fig. 2.10.1. Gammaherpesvirus accelerates reactivation from latency and increased virus replication in physiological oxygen tensions. MHV68 latently infected splenocytes from C57bl/6J mice (n=3) were collected and processed on 16 dpi. (A) Limiting dilution assay was performed on 21% O_2 or 1% O_2 to determine frequency of viral reactivation in low oxygen levels. At 63.2% the frequency reactivating splenocytes (dotted line) normoxia reactivation was 1 in 42,743 and from physioxic conditions 1 in 29,498. Symbols represent the mean percentage of wells positive for virus detection +/- standard error of the mean. Curve fit line were derived from nonlinear regression analysis. Data represents results of one experiment, performed in triplicates, out of more than three independent experiments. (B-C) Different ratios of splenocytes to 10^5 MEFs, (10^4 Left, 10^5 Center, 10^6 Right) were plated and incubated at 21% O_2 or 1% O_2. Graphs represent one out of two experiments. (B) Supernatants were collected, and viral titers were quantified by plaque assay on days 4, 5 and 6 post infection. *, $p<0.05$. **, $p<0.01$. ****, $p<0.001$. Statistical significance was determined by Multiple student's t-test (C) At 3 dpi, RNA was isolated from cell layer of co-cultures and RTA levels were measured by qRT-PCR. *, $p<0.05$. Statistical significance determined by Student's t-test.

We then examined whether hypoxia would increase the amount of virus produced during reactivation of latently infected cells. After MHV68 latency establishment in mice, explanted splenocytes were plated at three ratios on top of 1 X 10^5 MEFs and co-incubated at 21% O_2 or 1% O_2 levels. Supernatants were collected after 4, 5, and 6 days in culture then titered by plaque assay. On day 4, MHV68 virus was not detected in supernatants from normoxic conditions (21% O_2) within the limits of detection of the assay, regardless of the analyzed splenocytes-to-MEFs ratio. Even more, no virus was detected after 6 days in supernatants from the 1:10 splenocytes-to-MEFs ratio (**Figure 2.10.1B**-left). In contrast, infectious virus was already present at day 4 in all splenocytes-to-MEFs ratios reactivated in low oxygen conditions (**Figure 2.10.1B**). On day 5, supernatants from the 10:1 splenocytes-to-MEFs ratio cultured at 1% O_2 showed the most significant difference in viral titers, of up to 500-fold when compared to 21% O_2 (**Figure 2.10.1B-Right**). Supernatants from the 1:1 splenocytes-to-MEFs ratio also showed a 100-fold boost (**Figure 2.10.1B-center**).

Althought no virus production was detected in supernatants collected from either oxygen level condition on day 3, mRNA analysis by qPCR revealed a significantly higher

RTA expression in the cell layer from hypoxic conditions when normalized to normoxic reactivation, regardless of the splenocytes-to-MEFs ratio (**Figure 2.10.1C**). Thus, our data show that hypoxia provides cellular conditions that accelerate and enhance viral production during reactivation from latency in the B-cell lineage, the primary reservoir of gammaherpesviruses. This is aligned with our finding in Figure 2.9.2B, which shows that reactivation is impaired by the loss of HIF1α further reinforcing the idea that hypoxia and the HIF1α pathway plays a role in gammaherpesvirus reactivation from latency.

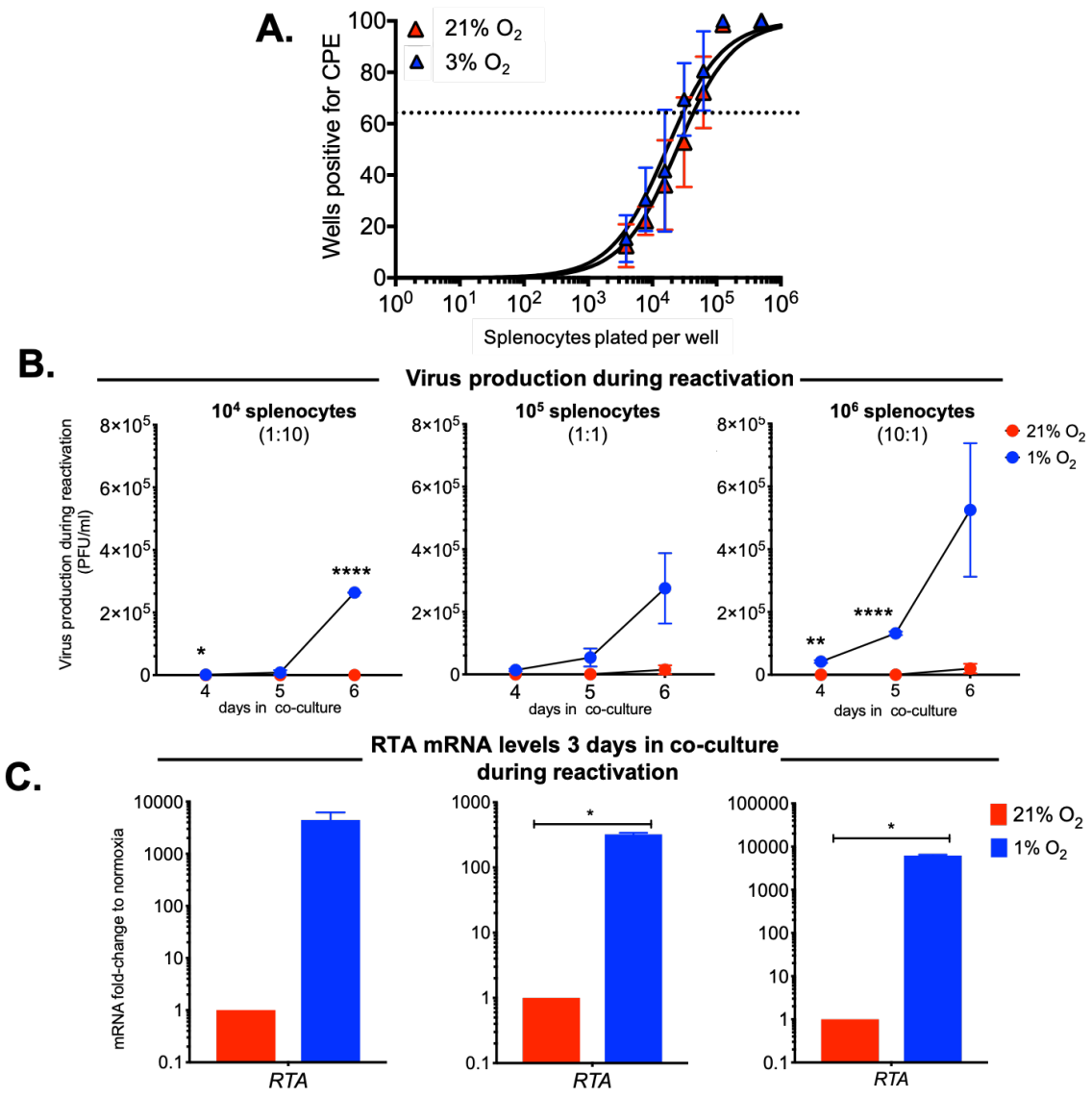

Fig. 2.10.2 Gammaherpesvirus accelerates reactivation from latency and increased virus replication in physiological oxygen tensions. MHV68 latently infected splenocytes from C57bl/6J mice (n=3) were collected and processed on 16 dpi. Limiting dilution assay was performed on 21% O_2 or 1% O_2 to determine frequency of viral reactivation in low oxygen levels. At 63.2% the frequency reactivating splenocytes (dotted line) normoxia reactivation was 1 in 42,743 and from physioxic conditions 1 in 29,498. Symbols represent the mean percentage of wells positive for virus detection +/- standard error of the mean. Curve fit line were derived from nonlinear regression analysis. (B-C) Different ratios of splenocytes to 10^5 MEFs, (10^4 Left, 10^5 Center, 10^6 Right) were plated and incubated at 21% O_2 or 1% O_2. Graphs represent one out of two experiments. (B) Supernatants were collected, and viral titers were quantified by plaque assay on days 4, 5 and 6 post infection. *, $p<0.05$. **, $p<0.01$. ****, $p<0.001$. Statistical significance was determined by Multiple student's t-test (C) At 3 dpi, RNA was isolated from cell layer of co-cultures and RTA levels were measured by qRT-PCR. *, $p<0.05$. Statistical significance determined by Student's t-test.

CHAPTER 3

MATERIALS AND METHODS

3.1. Mice

Mice containing germ line floxed exon 2 of HIF1α gene ($HIF1\alpha^{LoxP/LoxP}$) on a B6.129 background were purchased from Jackson Labs and together with age- and sex- matched with wild-type C57BL/6 J mice were bred and maintained at our institute animal facility. Female mice at 8- to 12-week-old were used in groups of three to nine in most experiments. The animal experiments described here were performed according to the approved protocol by the University of Miami Miller School of Medicine Institutional Animal Care and Use Committee. In addition, we report compliance with the ARRIVE guidelines as a requirement for reporting in vivo animal experiments.

3.2. Virus stock

MHV68 containing Cre-recombinase (MHV68-Cre) driven by human cytomegalovirus promoter and parental MHV68-BAC virus were kindly provided by Dr. Samuel Speck, Emory University, Atlanta. MHV68-WUMS strain was obtained from Dr. Herbert Virgin, University of Washington, St. Louis. Viral stocks were prepared by low MOI infection of 3T12 cells in 2% FBS complete medium. Virus stocks were harvested after 5 to 7 days of infection and were processed by a freeze-thawed cycle

followed by homogenization. Subsequently, virus lysate was purified by centrifugation at 1,000 rpm for 10 minutes, and the supernatant was filtered thru 0.4µm membrane to remove cell debris. Finally, purified virus stock was prepared by ultracentrifugation at 27,000 rpm for 1 hour at 4°C, and aliquots were transferred to -80°C for long-term storage. Viruses were quantified on 3T12 cells by standard plaque assay. Briefly, supernatants were diluted in 10-fold and transferred to cells layer in 24-well plates and incubated for 2 hours. 0.75% CMC containing overlay with 2% FBS complete media was added after inoculation. UV inactivation of viral stock was performed on a 60-mm plate in a Stratalinker, followed by plaque titration to ensure viral inactivation.

3.3. Cell culture

NIH 3T12 (ATCC CCL-164), a fibroblast cell line permissive to MHV68 replication was used to test the status of HIF1α after infection with MHV68-WUMS Strain. For all subsequent in vitro studies to test the absence of HIF1α activity, murine embryonic fibroblast (MEFs) were immortalized using the 3T3 NIH method. Briefly, MEFs were obtained from C57BL6 and B6. $HIF1\alpha^{2loxp}$ at 13.5 to 15.5 days post-coitus and cultured in T-25 flasks at $3X10^5$ cells every 3 days until passage 32. Immortalized $HIF1\alpha^{LoxP/LoxP}$ MEFs were

generated by lentiviral transduction of Cre-recombinase and selected by Blasticidin. MEFs and 3T12 were cultured at 37°C with 5% CO_2 in Dulbecco modified Eagle medium (DMEM) containing 10% fetal bovine serum (FBS), 2μM L-glutamine, 10μg/ml of gentamicin.

3.4. Low oxygen treatment

In experiments that required low oxygen concentration, cells were cultured in a humid hypoxia chamber under a mixture of O_2/ CO_2/ N_2. To obtain physiological oxygen concentrations or 3% O_2 conditions, 3:5:92 vol% and 1% O_2, 1:5:94 vol%. Hypoxia mimic was achieved by treatment with Cobalt chloride (Roche) at 150μM.

3.5. Excision assay

Cells were lysed in RLT buffer (Qiagen) supplemented with 1% β-mercaptoethanol and stored at -80°C before RNA extraction. RNA was isolated using RNeasy minikit (Qiagen), and cDNA was prepared using ImProm-II Reverse Transcription System (Promega) according to manufacturer's instruction. PCR conditions were as follow 95°C for 2 minutes followed by 32 cycles of 95 °C for 30 seconds, 64°C for 45 seconds and 72°C for 45 seconds. Excision was demonstrated by a shift in the size the mRNA fragment spanning exon 1 to exon 5 (600bp), which upon deletion of exon 2 can be detected in a 2.5 % DNA

agarose gel as a 400bp fragment when amplified by PCR (Invitrogen). Wild type MEFs isolated from C57Bl/6J mice transduced with the cre-recombinase expressing lentivirus was used as a control to detect the specificity of excision in floxed HIF MEFs. Primer sets were purchased from Sigma at follows: exon 1 forward 5′- CCGGCGGCGAGAAG -3′ and exon 5 reverse 5′- CCACGTTGCTGACTTGATGTTCAT- 3′.

3.6. Western blot

Samples were lysed in RIPA buffer and sonicated to avoid clumps from genomic DNA in lysates. Protein concentration was determined with BCA assay (Thermo Scientific) prior to resuspending in Laemmli buffer. 20 ug of protein lysates were separated by SDS-PAGE. Proteins were transferred to a PDVF membrane (Pall Life Sciences) at 100V for 1 hour at 4°C. The membrane was probed with 1:500 of mouse HIF1α antibody (Novus biologics) and 1: 2,000 mouse beta-actin antibody (Sigma). Primary antibodies were detected with HRP- conjugated anti-mouse secondary antibody (Sigma) and chemiluminescence reagent (Thermo Scientific).

3.7. Reporter assay

Transfection of 3T12 and MEFs were performed by using Lipofectamine 2000 following manufacturer's protocol. The HRE-Luciferase reporter is a pGL2 vector containing three

hypoxia response elements from the Pgk-1 gene upstream of firefly luciferase (Emerling et al. 2008). TK-Renilla (0.5 μg per well) and HRE-luciferase (0.5 μg per well) was co-transfected to control for transfection efficiency. After 12 hours of transfection, cells were infected with MHV68 at low MOI of (0.5 PFU/cell) and high MOI (3.0 PFU/cell). Firefly luciferase (F-Luc) activity in cell lysate was measured using Dual Luciferase Assay System (Promega Corporation), as recommended by the manufacturer. Renilla luciferase (R-Luc) activity in cell lysates was measured using 12 M coelenterazine in assay buffer (50 mM potassium phosphate, pH 7.4, 500 mM NaCl, 1 mM using a luminometer. Data are expressed in relative light units, and percentage of HIF1α dependent transcription was determined by normalizing luciferase units to Renilla.

3.8. Real-Time qPCR

Cells were lysed in RLT buffer (Qiagen) supplemented with 1% β-mercaptoethanol and stored at -80°C before RNA extraction. RNA was isolated using RNeasy minikit (Qiagen) and cDNA was prepared using ImProm-II Reverse Transcription System (Promega) according to manufacturer's instruction. Quantitative PCR was performed with 10 to 50 ng of cDNA using SyBr Green (Quanta Biosciences). PCR conditions were 95°C for

5 minutes followed by 45 cycles of 95 °C for 10 seconds, 60°C for 20 seconds and 72°C for 30 seconds. The TATA-binding site mRNA was used as the housekeeping gene. We compared the normalized Ct values (ΔCt) of each gene in two biological replicates between two groups of samples. All relative fold-change values were normalized against normoxic conditions using $2^{-\Delta\Delta Ct}$ to display fold-change

3.9. *In vitro* viral infections

Viral infections were performed in low volume serum-free complete media at 4°C for 2 hours at 21% O_2. Cell layers were washed twice with 1X PBS and then 2% FBS complete medium was added for experiments. For RNA and protein analysis, cell layer was washed once with cold 1X PBS.

3.10. Viral pathogenesis assays

Wild type and HIF1α-LoxP mice were euthanized with ketamine (100mg/kg) and xylazine (10mg/kg) and infected with $3x10^4$ PFU of MHV68-Cre virus. Lungs were removed on days 3, 5 and 7 post infection and freezed-thawed prior to processing. Tissue was disrupted in 1ml of 2% FBS complete medium using a handheld Omni homogenizer (www.OMNI-INC.com). Viral titers were determined by plaque assay on 3T12 cells plated in 24 well-plates and cultured in 0.75% CMC-overlay medium.

3.11. Limiting dilution assay

Bulk splenocytes were serially diluted by 2-fold on days 16 and 42 post infection after RBC lysis and plated on primary MEF starting at 1X 10^5 cells/well down to 7.5X10^2 cells/well with replicates of 24-well per dilution in 96-well plate. After 3 weeks, sups were collected and re-plated into 3T12 cells to amplify the virus and cytopathic effects was scored.

3.12. Viral genome frequency

Splenocytes were thawed and counted and diluted in 10^4 uninfected 3T12 cells. After proteinase K treatment, two rounds of PCR were performed against MHV68 ORF50. Copies of a plasmid containing ORF50 in 10, 1 and 0.1 copies were diluted against 1X10^4 3T12 cells and amplified in each run to ensure sensitivity of assay.

3.13. Virus reactivation of splenocytes in low oxygen

At day 16 following intranasal infection, (n=3) spleens were processed to obtain splenocytes at a single-cell suspension. Explanted splenocytes were plated at different quantities (10^4, 10^5 and 10^6) on top of a MEFs layer (1X10^5 cells per well) in a 6-well plate in duplicates. The-co-culture was kept in 2-ml of 2% FBS complete 1X DMEM media then transfer to 21% O_2 or 1% O_2 conditions.

3.14. Identification of HRE sequences within viral sequences

Computer-assisted prediction of HIF1α binding sites within the 500bp upstream of MHV68 ORFs was performed with TESS (Transcription Element Search System) using TRANSFAC for the search string RCGCT allowing only core position for strings with a maximum allowable string mismatch of %10.

3.15. Enzyme- linked immunosorbent assay

IL-1β and TNF-α were quantified by a mouse ELISA Ready-SET-Go! Kit (Affimetrix, eBioscience San Diego, CA). Plates were prepared and assayed according to the manufacturer's protocol and signals were read at 450 nm and subtracted the values of 570 nm to those of 450 nm.

3.16. Statistical analyses

Data analysis was perform using Prism software (Graphpad). Viral titer, reporter assays and mRNA fold-change were analyzed with a two-tailed Student t test and values are expressed as the means of standard error. Frequencies of reactivation and viral DNA positive cells were determined within the nonlinear regression fit of the results on the regression line that intersected at 63.2%, following a Poisson distribution. Results were considered to be statistically significant for values of $P<0.05$.

CHAPTER 4

DISCUSSION

Understanding the role of the HIF1 pathway in the viral life cycle of oncogenic gammaherpesviruses is currently hindered by the lack of a suitable infection model. We present cumulative data indicating the importance of HIF1α in MHV68 lytic replication and reactivation from latency. In this study, we show that MHV68 activates the HIF1 pathway and that knock-out of HIF1α transcriptional activity diminished lytic replication in vitro and in an in vivo model of HIF knock-out of infected cells. Moreover, this truncated form of HIF1α impaired lytic reactivation of cells latently infected in vivo.

We show that MHV68 infection increased HIF1α protein levels. This was coupled with an increase in HIF1α -dependent transcription activity (**Figure 2.1.1C**). A similar HIF upregulation was found in endothelial cells latently infected by KSHV (Carroll et al. 2006), an oncogenic gammaherpesvirus that encodes many genes with the potential to upregulate HIF1α (Morinet et al. 2013). Although, the MHV68 viral genome is structurally similar to KSHV with many of the viral homologous (Cesarman et al. 2019b) found to activate the HIF pathway in

KSHV are also present in MHV68 but, the exact mechanisms whereby the virus could target the HIF1 pathway are still to be defined. A recent report shows that MHV68 activates IKKβ, a recently discovered transcriptional activator of HIF1α during cellular defense against microbes (Dong et al. 2010; Rius et al. 2008).

To further define the role of HIF1α in replication we generated knock-out cells (**Figure 2.3.1**). We found that deletion of the DNA-binding motif impaired viral replication (**Figure 2.3.1A**). In searching for possible explanations for the decrease in viral replication, we analyzed the expression of viral HRE containing genes (**Figure 2.3.1B**) and found that in 7 of 17 viral gene mRNA levels were decreased in the HIF deleted (**Figure 2.3.1C**). Our findings confirmed the conserved HREs within ORF50 previously published (Polcicova et al. 2008). The majority of these HRE-containing viral genes have been described as essential for lytic replication such as DNA replication and assembly of mature virions (E. Barton, Mandal, and Speck 2011) (Supplementary Table 1). Out of these genes, particularly striking, was the downregulation of the KSHV homologous vGPCR gene in HIF1α Null Cells (**Figure 2.3.1B**). This is consistent with a recent report that also shows that KSHV vGPCR is a gene under strong regulation by

HIF1α (Singh et al. 2018). Since vGPCR is required for RTA gene and protein expression during lytic replication of KSHV (Bottero et al. 2009), it is possible that vGPCR downregulation in the absence of HIF1α would hinder RTA participation in lytic gene expression.

We found that the upregulation of glycolytic enzymes by MHV68 during normoxic infection was impaired by HIF1α deletion (**Figure 2.3.1D**). Metabolic reprogramming by gammaherpesviruses was also observed during KSHV and EBV de novo infection in vitro (Delgado et al. 2010b). Previous results published by our laboratory have demonstrated that treatment of MHV68 infected cells with 2-deoxy-D-glucose (2DG), a glycolytic inhibitor that was found inhibits the growth of KSHV-infected cells metabolically reprogrammed to glycolysis in normoxia (Delgado et al. 2010a), decreased by 5- fold of production of mature virions in comparison to untreated cells (Leung et al. 2012) pointing to a role of metabolic reprogramming involving HIF1α in MHV68 replication.

Recent studies have demonstrated that low oxygen tension can either enhance or downregulate virus infection (Hwang et al. 2006; Jiang et al. 2006). It is unknown whether low oxygen level influences gammaherpesvirus lytic replication in the absence of HIF1α. We found that MHV68 lytic program is more

heavily influenced by HIF1α under lower oxygen conditions—similar to physiological levels of oxygen in tissues and cells (Nathan and Singer 1999a). We found that at 3% oxygen levels, MHV68 in HIF1α Null cells undergo a further significant replication impairment concomitant to a higher decrease on viral gene expression (**Figure 2.8.2**). This could be the consequence of other transcription factors upregulated by an oxygen-depleted environment that could contribute to viral gene regulation (Cummins and Taylor 2005; Dalton-Griffin, Wilson, and Kellam 2009) but; more likely the fact that many non-HRE containing viral genes are regulated by HIF-regulated genes such as RTA. Taken together our in vitro results in 21% O_2 and 3% O_2 show that HIF1α plays an important role in MHV68 replication and that this is due, at least in part, by a key role in the regulation of viral gene transcription.

Infection of floxed transgenic mice with MHV68-Cre to knock-out HIF1α in vivo revealed that HIF1α is necessary for optimal viral expansion on the site of acute infection in the animal model. This is consistent with our data showing that HIF1α upregulation plays a role in MHV-68 de lytic infection by regulating its lytic genes. This could explain why the peak of viral titers are decreased in lungs (**Figure 2.9.1C and D**). It is also likely that a reduction in viral expansion

during the initial lytic phases in the lung could affect the extent of inflammation explaining the significant decrease of IL1β production in lungs lysates on day 7 (**Figure 2.9.1E**). These findings suggest that in the gammaherpesvirus life cycle, HIF1α is necessary for lytic virus expansion during acute infection of its host.

Similar to other herpesviruses, acute replication of gammaherpesviruses is followed by the long-term establishment of latent reservoirs in the host. Although the frequency of latency establishment shown by nested PCR of bulk splenocytes on day 16 (**Figure 2.9.2A**) was the same between wild type and HIF1αLoxP mice after MHV68-Cre virus infection, we found that the frequency of ex vivo reactivation of lytic virus from latently infected splenocytes was impaired in the absence of HIF1α (**Figure 2.9.2B**). To further establish a possible role of HIF1α in reactivation from latency, we tested WT virus reactivation in a lower oxygen context that we have shown increase HIF1α levels and activity. We found that low oxygen concentrations accelerated MHV68 reactivation and significantly increased the number of infectious virions released concomitant with viral RTA upregulation. Our data further points to a critical role of HIF in gammaherpesvirus infection as it is likely to affect not only viral replication

but viral reactivation in tissues where there is lower physiological oxygen level. It previously found that exposure of KSHV and EBV infected cells to hypoxic conditions can trigger a latent to lytic replication switch and enhance viral production and reactivation (D. A. Davis 2001; Jiang et al. 2006). This likely happens via interaction of HIF1α with the transcriptional machinery that regulates viral expression. In KSHV, the expression of the Replication and Transcription Activation (RTA) and a lytic gene cluster is enhanced by HIF1α in complex with viral-encoded proteins such as the Latency-Associated Nuclear Antigen (LANA) (Cai et al. 2006; Haque et al. 2006). Similarly, in EBV positive cell lines, HIF1α binds HREs located within the promoter region of the latent-lytic switch gene, BZLF1 (Kraus et al. 2017).

Both in KSHV and EBV, HIF1α has been linked to metabolic reprogramming of the host cell, modulation of viral latency, lytic replication, and tumorigenesis. Our work further contributes to the understanding of HIF1 pathway during the productive viral cycle in a natural infection and lytic replication in a cell and animal model. It establishes the utility of MHV68 as a model that can further our understanding of the mechanisms whereby gammaherpesviruses interact with oxygen-sensing pathways. Our data also opens up new avenues

to dissect the contribution of HIF1α in gammaherpesvirus infection of specific cell types such as myeloid and naïve and memory B cells that are targeted by MHV68 in vivo and can lead to lymphomagenesis under immunosuppression (Sunil-Chandra et al. 1994). Our findings demonstrate the importance of the interplay of the oxygen sensing machinery and gammaherpesviruses, which is key to understand their pathobiology.

CHAPTER 5

CONCLUSIONS AND FUTURE DIRECTIONS

The research findings presented here sets the ground for the mouse gammaherpesvirus MHV68 as a relevant model to study the mechanisms in which activation of the hypoxia-inducible factors regulate the replication and pathogenesis of gammaherpesviruses. These results demonstrated activation of HIF1α by an evolutionary relative and emphasize the role of HIF1α during the lytic life cycle of gammaherpesviruses during de novo infection and reactivation from latency. Moreover, this work demonstrates an impact of physiological oxygen concentrations in the gHV lytic cycle which results in the enhancement of virion production in the process.

Our findings demonstrating that exon 2 HIF1α deletion impairs lytic replication at lower, physiological, oxygen levels and that *ex vivo* reactivation in these conditions enhances virus production suggest the influence of physiological oxygen levels in the virus life cycle. A study by Richard Kraus *et al.* at the University of Wisconsin found that EBV positive cells further from blood vessels and lower oxygen levels, detected by a hypoxia-specific probe, expressed lytic reactivation and replication transcription factor (Kraus et al. 2017). Similar to EBV, and KSHV, we also

detected hypoxia-responsive sites throughout the genome which strongly suggest that low O_2 levels could dictate the expression of lytic genes. It is suggested that the lytic reactivation induced by differentiation of infected memory B cells into plasmablasts seeds the viral reservoir during long-term infection. It merits further investigation whether hypoxia-induced lytic reactivation in low oxygen environments could also support the pool of latently infected cells within its host during long-term infection.

The expression of Cre-recombinase under a MHV68 viral promoter poses technical limitations. Our conclusion that Cre expression and HIF1α excision occurred after accumulation of HIF1α could explain why there was no difference in genomic latency and the modest changes observed in reactivation. The construction of a recombinant MHV68 with immediate Cre-recombinase delivery specific to infection could drive inactivation of HIF1α before viral activation. Since the tegument-associated viral proteins exert immediate function upon viral entry, they present a feasible candidate for engineering a protein fusion to Cre-recombinase.

Finally, these findings encourages the use of MHV68 infection of a B cell-specific HIF1α mutant mice like the Mb1^{cre}HIF1αLoxP transgenic mouse (Meng et al. 2018). The *Mb1*

gene encodes the Ig-alpha signaling subunit of the BCR and is exclusively expresses in B cells during their early development (Hobeika et al. 2006). Upon characterization of these mice by Xianyi Meng *et al.*, published in Nature Communications, HIF1α deficiency in B-cells led to reduce numbers of a population of B1a ($CD1d^{hi}CD5^{+}$) B cells in the peritoneal cavity. However, cautious should be taken since a study published in Virology by Michaela Rekow *et al.* showed that peritoneal B-1 B cells harbor MHV68 DNA during long-term genomic latency (Rekow et al. 2016). HIF1α deficiency in B-cells also impairs production of IL-10, which plays an important role in the survival and proliferation of infected B cells and controls MHV68-specific $CD8^{+}$ T cells (Andrea M. Siegel, Herskowitz, and Speck 2008). In the latter, IL-10 expression is driven by the MHV68 specific gene M2. It is worth investigating whether M2 activates HIF1α and contribute to IL-10 production in B cells.

REFERENCES

Arvey, Aaron et al. 2012. "An Atlas of the Epstein-Barr Virus Transcriptome and Epigenome Reveals Host-Virus Regulatory Interactions." *Cell Host and Microbe* 12(2): 233–45.

Bais, C et al. 1998. "G-Protein-Coupled Receptor of Kaposi's Sarcoma-Associated Herpesvirus Is a Viral Oncogene and Angiogenesis Activator." *Nature* 391(6662): 86–89.

Barton, Erik, Pratyusha Mandal, and Samuel H Speck. 2011. "Pathogenesis and Host Control of Gammaherpesviruses: Lessons from the Mouse." *Annual Review of Immunology* 29: 351–97.

Barton, Erik S. et al. 2007. "Herpesvirus Latency Confers Symbiotic Protection from Bacterial Infection." *Nature* 447(7142): 326–29.

Bhatia, R et al. 2017. "Disseminated Kaposi's Sarcoma in a Human Immunodeficiency Virus-Infected Homosexual Indian Man." *Indian J Dermatol Venereol Leprol* 83(1): 78–83.

Bhatt, A. P. et al. 2012. "Dysregulation of Fatty Acid Synthesis and Glycolysis in Non-Hodgkin Lymphoma." *Proceedings of the National Academy of Sciences* 109(29): 11818–23.

Bortz, Eric et al. 2018. "Proteomics of Bronchoalveolar Lavage Fluid Reveals a Lung Oxidative Stress Response in Murine Herpesvirus-68 Infection." *Viruses* 10(12).

Bottero, Virginie et al. 2009. "Kaposi Sarcoma-Associated Herpes Virus (KSHV) G Protein-Coupled Receptor (VGPCR) Activates the ORF50 Lytic Switch Promoter: A Potential Positive Feedback Loop for Sustained ORF50 Gene Expression." *Virology* .

Cai, Qiliang et al. 2006. "Kaposi's Sarcoma-Associated Herpesvirus Latent Protein LANA Interacts with HIF-1 Alpha to Upregulate RTA Expression during Hypoxia: Latency Control under Low Oxygen Conditions." *Journal of Virology* 80(16): 7965–75.

Carroll, Patrick A, Heidi L Kenerson, Raymond S Yeung, and Michael Lagunoff. 2006. "Latent Kaposi's Sarcoma-Associated Herpesvirus Infection of Endothelial Cel Activates Hypoxia-Induced Factors." *Journal of Virology* 80(21): 10802–12.

Cavallin, Lucas E. et al. 2018. "KSHV-Induced Ligand Mediated Activation of PDGF Receptor-Alpha Drives Kaposi's Sarcomagenesis." *PLoS Pathogens* 14(7): 1–28.

Cesarman, Ethel. 2013. "Gammaherpesviruses and Lymphoproliferative Disorders." *Annual Review of Pathology: Mechanisms of Disease* 9(1): 349–72.

Cipková-Jarčušková, J et al. 2013. "Biological and Pathogenetic Characterization of Different Isolates of Murine Gammaherpesvirus 68 (MHV-68) in the Context of Study of Human Oncogenic Gammaherpesviruses." *Acta Virologica* 57(2): 105–12.

Collins, Christopher M. et al. 2012. "Tracking Murine Gammaherpesvirus 68 Infection of Germinal Center B Cells In Vivo" ed. J. Pedro Simas. *PLoS ONE* 7(3): e33230.

Cummins, Eoin P., and Cormac T. Taylor. 2005. "Hypoxia-Responsive Transcription Factors." *Pflügers Archiv* 450(6): 363–71.

Dalton-Griffin, Lucy, Sam J Wilson, and Paul Kellam. 2009. "X-Box Binding Protein 1 Contributes to Induction of the Kaposi's Sarcoma-Associated Herpesvirus Lytic Cycle under Hypoxic Conditions." *Journal of Virology* 83(14): 7202–9.

Damania, Blossom. 2007. "Chapter 61 EBV and KSHV – Related Herpesviruses in Non-Human Primates Lymphocryptoviruses of Old World Monkeys." *Human Herpesviruses: Biology, Therapy, and Immunoprophylaxis.* https://www.ncbi.nlm.nih.gov/books/NBK47448/.

Darekar, Suhas et al. 2012. "Epstein-Barr Virus Immortalization of Human B-Cells Leads to Stabilization of Hypoxia-Induced Factor 1 Alpha, Congruent with the Warburg Effect" ed. Sai Wah Tsao. *PLoS ONE* 7(7): e42072.

Davis, D. A. 2001. "Hypoxia Induces Lytic Replication of Kaposi Sarcoma-Associated Herpesvirus." *Blood* 97(10): 3244–50.

Delgado, Tracie et al. 2010a. "Induction of the Warburg Effect by Kaposi's Sarcoma Herpesvirus Is Required for the Maintenance of Latently Infected Endothelial Cells." *Proceedings of the National Academy of Sciences of the United States of America* 107(23): 10696–701.

Doherty, P C et al. 2001. "Dissecting the Host Response to a Gamma-Herpesvirus." *Philosophical transactions of the Royal Society of London. Series B, Biological Sciences* 356(1408): 581–93.

Dong, Xiaonan et al. 2010. "Murine Gamma-Herpesvirus 68 Hijacks MAVS and IKKbeta to Initiate Lytic Replication." ed. Klaus Früh. *PLoS Pathogens* 6(7): e1001001.

Dutia, Bernadette M et al. 2009. "A Novel Cre Recombinase Imaging System for Tracking Lymphotropic Virus Infection in Vivo." ed. Philip G. Stevenson. *PloS ONE* 4(8): e6492.

Efstathiou, S. et al. 1990. "Murine Herpesvirus 68 Is Genetically Related to the Gammaherpesviruses Epstein-Barr Virus and Herpesvirus Saimiri." *Journal of General Virology* 71(6): 1365–72.

Efstathiou, S., Y. M. Ho, and A. C. Minson. 1990. "Cloning and Molecular Characterization of the Murine Herpesvirus 68 Genome." *Journal of General Virology* 71(6): 1355–64.

Emerling, Brooke M et al. 2008. "PTEN Regulates P300-Dependent Hypoxia-Inducible Factor 1 Transcriptional Activity through Forkhead Transcription Factor 3a (FOXO3a)." *Proceedings of the National Academy of Sciences of the United States of America* 105(7): 2622–27.

Epstein, Andrew C.R. et al. 2001. "C. Elegans EGL-9 and Mammalian Homologs Define a Family of Dioxygenases That Regulate HIF by Prolyl Hydroxylation." *Cell* 107: 43–54.

Fickenscher, Helmut, and Bernhard Fleckenstein. 2001. "Herpesvirus Saimiri." *Philosophical Transactions of the Royal Society B: Biological Sciences* 356(1408): 545–67.

Fields, Bernard N., and David Mahan Knipe. 2013. *Fields VIrology*. Wolters Kluwer, Lippincott Williams & Wilkins.

Flaño, Emilio, In-Jeong Kim, David L Woodland, and Marcia A Blackman. 2002. "Gamma-Herpesvirus Latency Is Preferentially Maintained in Splenic Germinal Center and Memory B Cells." *The Journal of Experimental Medicine* 196(10): 1363–72.

François, Sylvie et al. 2013. "Illumination of Murine Gammaherpesvirus-68 Cycle Reveals a Sexual Transmission Route from Females to Males in Laboratory Mice." *PLoS Pathogens* 9(4): e1003292.

Greer, Samantha N et al. 2012. "The Updated Biology of Hypoxia-Inducible Factor." *The EMBO Journal* 31(11): 2448–60.

Habermann, Thomas M et al. 2018. "Clinical Characteristics and Outcomes of an Analysis of a Single Institution Experience of the 2017 World Health Organization (WHO) Classification of Post-Transplant Lymphoproliferative Disorders (PTLD)." *Blood* 132(Suppl 1): 456 LP – 456.

Haque, Muzammel et al. 2006. "Genetic Organization and Hypoxic Activation of the Kaposi's Sarcoma-Associated Herpesvirus ORF34-37 Gene Cluster." *Journal of Virology* 80(14): 7037–51.

Haque, Muzammel, and Konstantin G Kousoulas. 2013. "The Kaposi's Sarcoma-Associated Herpesvirus ORF34 Protein Binds to HIF-1α and Causes Its Degradation via the Proteasome Pathway." *Journal of Virology* 87(4): 2164–73.

Hobeika, E. et al. 2006. "Testing Gene Function Early in the B Cell Lineage in Mb1-Cre Mice." *Proceedings of the National Academy of Sciences of the United States of America* 103(37): 13789–94.

Huang, Yan et al. 2012. "Normal Glucose Uptake in the Brain and Heart Requires an Endothelial Cell-Specific HIF-1α-Dependent Function." *Proceedings of the National Academy of Sciences of the United States of America* 109(43): 17478–83.

Hughes, D. J., A. Kipar, J. T. Sample, and J. P. Stewart. 2010. "Pathogenesis of a Model Gammaherpesvirus in a Natural Host." *Journal of Virology*.

Hwang, Irene I L, Ian R Watson, Sandy D Der, and Michael Ohh. 2006. "Loss of VHL Confers Hypoxia-Inducible Factor (HIF)-Dependent Resistance to Vesicular Stomatitis Virus: Role of HIF in Antiviral Response." *Journal of Virology* 80(21): 10712–23.

Jham, Bruno C et al. 2011. "Amplification of the Angiogenic Signal through the Activation of the TSC/MTOR/HIF Axis by the KSHV VGPCR in Kaposi's Sarcoma." *PloS ONE* 6(4): e19103.

Jiang, Ju Hong et al. 2006. "Hypoxia Can Contribute to the Induction of the Epstein-Barr Virus (EBV) Lytic Cycle." *Journal of Clinical Virology* 37(2): 98–103.

Kietzmann, Thomas, Daniela Mennerich, and Elitsa Y. Dimova. 2016. "Hypoxia-Inducible Factors (HIFs) and Phosphorylation: Impact on Stability, Localization, and Transactivity." *Frontiers in Cell and Developmental Biology*.

Koh, Mei Y et al. 2008. "Molecular Mechanisms for the Activity of PX-478 , an Antitumor Inhibitor of the Hypoxia-Inducible Factor-1 A." *Mol Cancer Ther* 7(1): 90–101.

Kondo, Satoru et al. 2006. "EBV Latent Membrane Protein 1 Up-Regulates Hypoxia-Inducible Factor 1alpha through Siah1-Mediated down-Regulation of Prolyl Hydroxylases 1 and 3 in Nasopharyngeal Epithelial Cells." *Cancer Research* 66(20): 9870–77.

Kraus, Richard J. et al. 2017. "Hypoxia-Inducible Factor-1 Alpha Plays Roles in Epstein-Barr Virus's Natural Life Cycle and Tumorigenesis by Inducing Lytic Infection through Direct Binding to the Immediate-Early BZLF1 Gene Promoter." *PLOS Pathogens* 13(6): e1006404.

Leung, Howard J et al. 2012. "Activation of the Unfolded Protein Response by 2-Deoxy-D-Glucose Inhibits Kaposi's Sarcoma-Associated Herpesvirus Replication and Gene Expression." *Antimicrobial Agents and Chemotherapy* 56(11): 5794–5803.

Liang, Xiaozhen et al. 2011. "Murine Gamma-Herpesvirus Immortalization of Fetal Liver-Derived b Cells Requires Both the Viral Cyclin d Homolog and Latency-Associated Nuclear Antigen." *PLoS Pathogens* 7(9): 1–12.

Luo, Weibo, and Gregg L Semenza. 2011. "Pyruvate Kinase M2 Regulates Glucose Metabolism by Functioning as a Coactivator for Hypoxia-Inducible Factor 1 in Cancer Cells." *Oncotarget* 2(7): 551–56.

Ma, Qi et al. 2009. "Antitumorigenesis of Antioxidants in a Transgenic Rac1 Model of Kaposi's Sarcoma." *Proceedings of the National Academy of Sciences of the United States of America* 106(21): 8683–88.

Ma, Tao et al. 2015a. "KSHV Induces Aerobic Glycolysis and Angiogenesis through HIF-1-Dependent Upregulation of Pyruvate Kinase 2 in Kaposi's Sarcoma." *Angiogenesis* 18(4): 477–88.

Maral, Tugrul. 2000. "The Koebner Phenomenon in Immunosuppression-Related Kaposi's Sarcoma." *Annals of Plastic Surgery* 44(6): 646–48.

McGeoch, Duncan J. et al. 1995. "Molecular Phylogeny and Evolutionary Timescale for the Family of Mammalian Herpesviruses." *Journal of Molecular Biology* 247(3): 443–58.

McHugh, Donal et al. 2017. "Persistent KSHV Infection Increases EBV-Associated Tumor Formation *In Vivo* via Enhanced EBV Lytic Gene Expression." *Cell Host and Microbe* 22(1): 61-73.e7.

Meng, Xianyi et al. 2018. "Hypoxia-Inducible Factor-1α Is a Critical Transcription Factor for IL-10-Producing B Cells in Autoimmune Disease." *Nature Communications* 9(1).

Mesri, Enrique A, Mark A Feitelson, and Karl Munger. 2014. "Human Viral Oncogenesis: A Cancer Hallmarks Analysis." *Cell Host & Microbe* 15(3): 266–82.

Mesri, Enrique, Ethel Cesarman, and Chris Boshoff. 2010. "Kaposi's Sarcoma and Its Associated Herpesvirus." *Nature reviews. Cancer* 10(10): 707–19.

Morinet, Frédéric et al. 2013. "Oxygen Tension Level and Human Viral Infections." *Virology* 444(1): 31–36.

Moser, Janice M et al. 2005. "Role of B-Cell Proliferation in the Establishment of Gammaherpesvirus Latency." *Journal of Virology* 79(15): 9480–91.

Movafagh, Shahrzad, Sean Crook, and Kim Vo. 2015. "Regulation of Hypoxia-Inducible Factor-1a by Reactive Oxygen Species: New Developments in an Old Debate." *Journal of Cellular Biochemistry* 116(5): 696–703.

Mutlu, Agata D'Agostino et al. 2007. "In Vivo-Restricted and Reversible Malignancy Induced by Human Herpesvirus-8 KSHV: A Cell and Animal Model of Virally Induced Kaposi's Sarcoma." *Cancer Cell* 11(3): 245–58.

Myoung, Jinjong, and Don Ganem. 2011a. "Generation of a Doxycycline-Inducible KSHV Producer Cell Line of Endothelial Origin: Maintenance of Tight Latency with Efficient Reactivation upon Induction." *Journal of Virological Methods* 174(1–2): 12–21.

Nash, A A, B M Dutia, J P Stewart, and A J Davison. 2001. "Natural History of Murine Gamma-Herpesvirus Infection." *Philosophical transactions of the Royal Society of London. Series B, Biological Sciences* 356(1408): 569–79.

Nathan, A T, and M Singer. 1999a. "The Oxygen Trail: Tissue Oxygenation." *British Medical Bulletin* 55(1): 96–108.

Oksenhendler, Eric et al. 2002. "High Incidence of Kaposi Sarcoma-Associated Herpesvirus-Related Non-Hodgkin Lymphoma in Patients with HIV Infection and Multicentric Castleman Disease." *Blood* 99(7): 2331–36.

Polcicova, Katarina et al. 2008. "Up-Regulation of Murid Herpesvirus 4 ORF50 by Hypoxia: Possible Implication for Virus Reactivation from Latency." *Virus Research* 132(1–2): 257–62.

Rao, P., H. Jiang, and F. Wang. 2000. "Cloning of the Rhesus Lymphocryptovirus Viral Capsid Antigen and Epstein-Barr Virus-Encoded Small RNA Homologues and Use in Diagnosis of Acute and Persistent Infections." *Journal of Clinical Microbiology* 38(9): 3219–25.

Reese, T. A. et al. 2014. "Helminth Infection Reactivates Latent -Herpesvirus via Cytokine Competition at a Viral Promoter." *Science* 345(6196): 573–77.

Rekow, Michaela M et al. 2016. "Gammaherpesvirus Targets Peritoneal B-1 B Cells for Long-Term Latency." *Virology*: 140–44.

Rius, Jordi et al. 2008. "NF-KappaB Links Innate Immunity to the Hypoxic Response through Transcriptional Regulation of HIF-1alpha." *Nature* 453(7196): 807–11.

Sarawar, S R et al. 1996. "Cytokine Production in the Immune Response to Murine Gammaherpesvirus 68 . Cytokine Production in the Immune Response to Murine Gammaherpesvirus 68." *Journal of Virology* 70(5).

Sarawar, Sally R. et al. 2002. "Chemokine Induction and Leukocyte Trafficking to the Lungs during Murine Gammaherpesvirus 68 (MHV-68) Infection." *Virology* 293(1): 54–62.

Sarosiek, K. A. et al. 2010. "Efficacy of Bortezomib in a Direct Xenograft Model of Primary Effusion Lymphoma." *Proceedings of the National Academy of Sciences* 107(29): 13069–74.

Scholz, Barbara A. et al. 2013. "Abortive Lytic Reactivation of KSHV in CBF1/CSL Deficient Human B Cell Lines." *PLoS Pathogens* 9(5).

Semenza, G L. 1999. "Regulation of Mammalian O2 Homeostasis by Hypoxia-Inducible Factor 1." *Annual Review of Cell and Developmental Biology* 15: 551–78.

Shin, Young C et al. 2008. "Kaposi's Sarcoma-Associated Herpesvirus Viral IFN Regulatory Factor 3 Stabilizes Hypoxia-Inducible Factor-1 Alpha to Induce Vascular Endothelial Growth Factor Expression." *Cancer Research* 68(6): 1751–59.

Shrestha, Prabha et al. 2017. "Hypoxia-Inducible Factor-1 Alpha as a Therapeutic Target for Primary Effusion Lymphoma." *PLoS Pathogens* 1: 1–20.

Siegel, A. M., U. S. Rangaswamy, R. J. Napier, and S. H. Speck. 2010. "Blimp-1-Dependent Plasma Cell Differentiation Is Required for Efficient Maintenance of Murine Gammaherpesvirus Latency and Antiviral Antibody Responses." *Journal of Virology* 84(2): 674–85.

Siegel, Andrea M., Jeremy H. Herskowitz, and Samuel H. Speck. 2008. "The MHV68 M2 Protein Drives IL-10 Dependent B Cell Proliferation and Differentiation." *PLoS Pathogens* 4(4).

Singh, Rajnish Kumar et al. 2018. “Metabolic Reprogramming of Kaposi ’ s Sarcoma Associated Herpes Virus Infected B-Cells in Hypoxia.” *PLoS Pathogens* 14(5): 1–28.

Sodhi, Akrit et al. 2000. “The Kaposi’s Sarcoma-Associated Herpes Virus G Protein-Coupled Receptor Up-Regulates Vascular Endothelial Growth Factor Expression and Secretion through Mitogen-Activated Protein Kinase and P38 Pathways Acting on Hypoxia-Inducible Factor 1 Alpha.” *Cancer Res.* 60(17): 4873–80.

Song, M. J. et al. 2005. “Identification of Viral Genes Essential for Replication of Murine -Herpesvirus 68 Using Signature-Tagged Mutagenesis.” *Proceedings of the National Academy of Sciences* 102(10): 3805–10.

Stevenson, Philip G, Janet S May, Viv Connor, and Stacey Efstathiou. 2010. “Vaccination against a Hit-and-Run Viral Cancer.” *The Journal of General Virology* 91(Pt 9): 2176–85.

Suárez, Andrea Luísa, and Linda Faye van Dyk. 2008. “Endothelial Cells Support Persistent Gammaherpesvirus 68 Infection.” ed. Jae U. Jung. *PLoS Pathogens* 4(9): e1000152.

Sunil-Chandra, N. P., S. Efstathiou, J. Arno, and A. A. Nash. 1992. “Virological and Pathological Features of Mice Infected with Murine Gammaherpesvirus 68.” *Journal of General Virology*.

Sunil-Chandra, N P, J Arno, J Fazakerley, and a a Nash. 1994. “Lymphoproliferative Disease in Mice Infected with Murine Gammaherpesvirus 68.” *The American Journal of Pathology* 145(4): 818–26.

Tang, Nan et al. 2004. “Loss of HIF-1alpha in Endothelial Cells Disrupts a Hypoxia-Driven VEGF Autocrine Loop Necessary for Tumorigenesis.” *Cancer Cell* 6(5): 485–95.

Veeranna, Ravindra P et al. 2012. “Kaposi’s Sarcoma-Associated Herpesvirus Latency-Associated Nuclear Antigen Induction by Hypoxia and Hypoxia-Inducible Factors.” *Journal of Virology* 86(2): 1097–1108.

Wakisaka, Naohiro et al. 2004. "Epstein-Barr Virus Latent Membrane Protein 1 Induces Synthesis of Hypoxia-Inducible Factor 1 α." *Mol Cell Biol* 24(12): 5223–34.

Webster-Cyriaque, Jennifer. 2002. "Development of Kaposi's Sarcoma in a Surgical Wound." *N Engl J Med* 346(16): 1207–10.

Weck, K E et al. 1996. "Mature B Cells Are Required for Acute Splenic Infection, but Not for Establishment of Latency, by Murine Gammaherpesvirus 68." *Journal of Virology* 70(10): 6775–80.

Weck, K E, S S Kim, I V Virgin HW, and S H Speck. 1999. "B Cells Regulate Murine Gammaherpesvirus 68 Latency." *Journal of Virology* 73(6): 4651–61.

Yarchoan, Robert, David A. Davis, and Andrea S. Rinderknecht. 2002. "Development of Kaposi's Sarcoma at the Site of a Bipsy." *N Engl J Med* 347(10): 763–64.

Yogev, Ohad, Dimitris Lagos, Tariq Enver, and Chris Boshoff. 2014. "Kaposi's Sarcoma Herpesvirus MicroRNAs Induce Metabolic Transformation of Infected Cells." *PLoS Pathogens* 10(9): e1004400.

Zhang, Liming et al. 2014a. "Inhibition of KAP1 Enhances Hypoxia-Induced Kaposi's Sarcoma-Associated Herpesvirus Reactivation through RBP-Jκ." *Journal of Virology* 88(12): 6873–84.